ESD-TR-66-249

Technical Note

1966-37

Off-Line Signal Processing Results for the Large Aperture Seismic Array

J. Capon
R. J. Greenfield
R. T. Lacoss

11 July 1966

Prepared for the Advanced Research Projects Agency
under Electronic Systems Division Contract AF 19(628)-5167 by

Lincoln Laboratory
MASSACHUSETTS INSTITUTE OF TECHNOLOGY
Lexington, Massachusetts

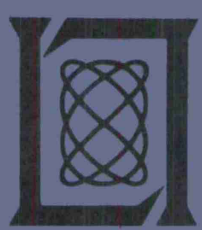

The work reported in this document was performed at Lincoln Laboratory, a center for research operated by Massachusetts Institute of Technology. This research is a part of Project Vela Uniform, which is sponsored by the U.S. Advanced Research Projects Agency of the Department of Defense; it is supported by ARPA under Air Force Contract AF 19(628)-5167 (ARPA Order 512).

MASSACHUSETTS INSTITUTE OF TECHNOLOGY

LINCOLN LABORATORY

OFF-LINE SIGNAL PROCESSING RESULTS FOR THE LARGE APERTURE SEISMIC ARRAY

J. CAPON

R. J. GREENFIELD

R. T. LACOSS

Group 64

TECHNICAL NOTE 1966-37

11 JULY 1966

LEXINGTON MASSACHUSETTS

ABSTRACT

The results of a series of off-line signal processing experiments are presented for the experimental Large Aperture Seismic Array (LASA) located in eastern Montana. In particular, the signal-to-noise ratio gains achievable by maximum-likelihood processing, as well as other simpler forms of processing, are given as a function of frequency, aperture, and number of sensors. A partial discussion of the physical characteristics of the noise field which led to these results is also presented.

The spurious precursor introduced by one form of signal processing, and shown to be caused primarily by the signal amplitude scatter within a subarray, can be effectively reduced by using amplitude equalization. The signal amplitude scatter within a subarray, and between subarrays, is thus found not to degrade seriously the performance of the signal processing. In fact, the scatter of amplitudes between subarrays, which is significantly larger than that within a subarray, is a definite asset.

It was found that the effectiveness of the processing depends not only on the array spatial filtering ability, but on differences in absolute level of the noises in the various sensors. Long-period array data from the extended TFO array were processed and showed roughly $\sqrt{N}$ improvement.

Our experience in processing a number of events is illustrated by a discussion of the results obtained on two particularly weak events with the maximum-likelihood filter. The apparent magnitude of one event (as averaged over the LASA) was 3.5, and that of the other was 4.0. It was found that the processing was capable of extracting both events from the background noise to the extent that they could be identified as earthquakes and not nuclear explosions. An experiment in suppressing large events that obscure simultaneous smaller events from other source regions is reported.

On the basis of these results, several recommendations concerning off-line and on-line processing methods and array geometry are given.

Accepted for the Air Force
Franklin C. Hudson
Chief, Lincoln Laboratory Office

TABLE OF CONTENTS

I. INTRODUCTION

This report discusses the results of an extensive investigation of various methods of improving signal-to-noise ratio (SNR) by combining the individual sensor outputs of the experimental Large Aperture Seismic Array[1-4] in Montana. There were four objectives in our investigation. The first was to select forms of array processing that were simple enough to be implemented in on-line digital equipment for detecting and locating seismic events at as low a threshold magnitude as possible. The second was to determine how much additional gain in SNR could be achieved by off-line processing of recorded data if computing complexity and time were not a limitation. The third objective was to learn whether an array geometry different from the one used in Montana might produce better results, and finally we were interested in inferring the physical characteristics of the noise field.

The family of three linear array processing schemes we have used is described in detail elsewhere.[5] The simplest is delay-and-sum, which we will refer to here as DS processing, in which only a steering delay is applied to each seismometer output before summation. This procedure steers the main lobe but makes no attempt to steer sidelobes and nulls for further noise minimization. The next scheme in order of complication, weighted delay-and-sum or WDS, attempts to do just this by applying an amplitude coefficient to each element in addition to the steering delay. The most complicated of the three methods, filter-and-sum or FS, establishes a delay and amplitude weight for each element at each resolvably different frequency by attaching a filter to each element and then summing filter outputs.

In our work the delays, weights, and filtering and summing operations were synthesized on a computer. The particular amplitude weighting coefficients for WDS and the filter functions for FS were designed from noise data observed over a several-minute period called the fitting interval. Our particular approach to the design of these parameters is the maximum-likelihood method[5] and we shall frequently refer to FS processing by that name. Maximum-likelihood processing has the feature that it produces an output trace in which no frequency distortion is imposed on the signal seismogram waveform. For off-line processing the fitting interval is usually chosen to be at a time adjacent to the onset of the event; for on-line processing it is not usually possible to update these parameters very often.[6]

In the synthesis procedures just described for WDS and FS there is a finite number of coefficients to be determined, i.e., degrees of freedom in the processing. For WDS this is equal to the number of seismometers, (NS), for FS it is equal to the number of seismometers times the number of parameters (NFP) that specify each filter function. The synthesis procedure will deploy these available degrees of freedom to minimize whatever noise is apparent in the set of traces observed in the fitting interval. Therefore it makes a great deal of difference whether or not the traces have been prefiltered. Prefiltering operations are quite effective in suppressing noise lying outside the signal band, but extreme care must be exercised lest weak but important features of the seismogram be distorted.

Three forms of prefilters were used in our studies (1) no prefilter, (2) a "bandpass prefilter" (Fig. 1A) in the $0.6 - 2.0$ cps range, and (3) a "notch filter"

(Fig. 1B) designed to suppress microseisms in the 0.2 – 0.3 cps range. The unprefiltered condition is important particularly for preserving waveform features at the longer period range (below 0.6 cps) such as S-phases[7] and longer period P-signals. The bandpass prefilter badly distorts first motion, but is suitable for complexity measurements and for pP observations. The notch prefilter is preferable when observing first motion.

It should be mentioned that in actually carrying out off-line processing it is customary for an analyst to examine the traces to be combined and delete those occasional ones which have an event which is smaller by about 6 db or more than the average of those traces which are to be processed. If this is done, the amount of signal amplitude loss in the final processed output trace is rarely more than 1.5 to 2.0 db. This factor will therefore be ignored in most of what follows.

We proceed now to a discussion of our results on the tradeoffs between many different factors involved in array processing.

II. PARAMETERS USED IN THE DESIGN OF THE MAXIMUM-LIKELIHOOD FILTER

The data were obtained from recordings of short-period vertical seismometers at LASA that were sampled every 1/20 second. The basic assumption in the design of the maximum-likelihood filter (by which we mean the set of individual filters) is that the event propagates across the array as a plane wave so that the signal in each sensor is the same except possibly for a time delay. The noise characteristics are estimated in the fitting interval and an FS filter is synthesized on the basis of this measurement. The filter synthesis is performed by evaluating the NFP weighting coefficients of a convolutional filter for each of the NS sensors used, where NFP denotes number of filter points.

The important variable parameters used in the design of the maximum-likelihood filter, given a certain NS and a fixed array geometry, are the length of the fitting interval, NFP, and NIM, where every NIM^{th} data point is used in the fitting interval to estimate noise characteristics. It was found that the optimum choice of NIM was 2. That is, every other sample was used in the fitting interval corresponding to a sampling rate of 10 cps and a foldover frequency of 5 cps. NIM did not need to be less than 2 because it was found that there was very little noise energy above 5 cps, and a larger value for NIM tended to lead to serious aliasing due to frequency foldover. The length of the fitting interval was set at three minutes as a compromise between stability of the estimates of noise characteristics and computation time. A value of NFP = 21, corresponding to a filter length of two seconds, was chosen as a compromise among several factors. The filter length should be made long enough to effectively filter the noise.

However, the signals in the sensors within the various subarrays tend to be identical, after the time-delay correction, for about two seconds. In addition, the computer time requirements become excessive if NFP is too large.

A number of computer runs were made to substantiate the choice of these parameters. Figure 2 shows signal-to-noise ratio gain in the fitting interval as a function of the number of filter points. Figure 2A is for the unprefiltered condition and Fig. 2B for the situation in which the 25 traces have been bandpass prefiltered. Along the lower curve the filters are physically realizable, i.e., the sum of the impulse responses of the 25 sensors is zero for all values of delay except the first one at which the sum is unity, so that the filter operates on the basis of only past samples of the noise. Along the top curve the filters are two-sided, i.e., the sum of the impulse responses is zero except at the center sample point at which they sum to unity, so that the two-sided filter operates on the basis of the future as well as the past values of the noise. Since a response before excitation is implied, the two-sided filters are said to be physically unrealizable. The other points represent unrealizable filters whose build-up point is intermediate to that of the realizable filter and two-sided filter. The results show the superiority of the two-sided filter in yielding a high signal-to-noise ratio gain over the other filters. It is for this reason that the two-sided filter is used in all the processing of the various events reported here. However, one hazard in using an unrealizable filter is the possibility of an unwanted precursor in the output trace due to the fact that the signals are not identical in each of the sensors. This problem has been found to be manageable and will be discussed in Section V.

Unfortunately, the signal-to-noise ratio gain developed by the filter tends to drop outside of the fitting interval due to the sensitivity of the filter to the noise stationarity assumption. The data for this using unprefiltered traces are given in Fig. 3 for various NFP and fitting interval lengths. The time-domain synthesis refers to the early version of the maximum-likelihood filter synthesis program and the frequency-domain synthesis refers to the later version which is currently used. The frequency-domain synthesis has the advantage with respect to the time-domain synthesis of requiring much less computer time to synthesize the filter. For example, if NFP = 21, and 25 sensors are processed using a three-minute fitting interval, the respective 7094 running times are 10 minutes and 45 minutes. It is also seen from Fig. 3 that the frequency-domain synthesis is less sensitive to the assumption of noise stationarity than the time-domain synthesis. However, the signal-to-noise ratio gain of the frequency-domain filter is about 2 db less than that of the time-domain filter outside the fitting interval.

The manner in which the signal-to-noise ratio gain varies outside the fitting interval, for very long time intervals (days) as well as short time intervals (minutes) is shown in Fig. 4 for various forms of prefiltering. The results indicate that the noise is nonstationary so that the filter must be designed anew each time an event is processed. The rate of loss outside the fitting interval is not a strong function of frequency as will be seen in connection with Fig. 13.

It might be inferred from Fig. 2 that the signal-to-noise ratio gain could be made high by increasing NFP. That this is not the case is illustrated in Fig. 5. Due to the drop in signal-to-noise ratio gain outside the fitting interval, the gain cannot be

made any larger than what it would be for roughly NFP = 21, for both unfiltered and bandpass prefiltered raw data traces. These same results were verified on another event. It should be mentioned that these results were obtained with the time-domain program. The corresponding results for the frequency-domain program both inside and outside the fitting interval tend to agree with the lower curve in each pair in Fig. 5, i.e., the curves which indicate the gain outside the fitting interval for the time-domain synthesized filters.

III. SIGNAL-TO-NOISE RATIO GAIN VS NUMBER OF SENSORS AND APERTURE

A number of computer runs were made to determine signal-to-noise ratio gain vs number of sensors for both unfiltered and prefiltered traces and for the three forms of processing, FS, WDS, and DS. The results are shown in Figs. 6 and 7 for bandpass prefiltered and unprefiltered data, respectively. The three lines emanating from the FS gain figures for 25 sensors indicate the results of combining the respective subarray output traces by FS, WDS, and DS. It is seen that at this stage of processing there is very little difference between these three forms of processing as they all yield approximately $\sqrt{N}$-type gain. This result is also verified subsequently in Figs. 9 and 21.

Figure 8 summarizes the results of two separate experiments designed to determine the effect of both aperture and number of sensors on the signal-to-noise ratio gain for unfiltered traces. In the first experiment, indicated by the shaded bars, the FS outputs from four subarrays arranged in rings of various diameters or apertures, were combined by DS, WDS, and FS. The gains in the fitting interval for combining 21 subarray FS traces on this particular event were 35 db for DS, 36 for WDS and 38 for FS. It is seen from Fig. 8 that the signal-to-noise ratio gains for all three forms of processing groups of four subarrays tend to remain relatively independent of the aperture, and not very different at each aperture, indicating that the processed noise field is independent between subarrays. Figure 9 shows that DS combining of N subarray straight sums yields a roughly $\sqrt{N}$ noise suppression indicating that the straight sum traces are independent between subarrays.

In the second experiment, indicated by the unshaded bars, 25 sensors forming arrays of various apertures were drawn from the 525 available and processed by DS,

WDS, and FS. It is seen that DS and WDS did not perform competitively until the aperture reached about 20 km. The gain for FS began to deteriorate for apertures larger than one subarray diameter. These results indicate that with unfiltered traces FS is very useful within a subarray of diameter between 7 and 20 km and that for greater apertures simpler schemes will suffice.

The variation of the gain of WDS with number of sensors is shown in Fig. 10 for both unfiltered and bandpass prefiltered data. It was not possible to perform this experiment for FS because of the limitations imposed by the machine storage requirements of such a program. The results of Fig. 10 were obtained by distributing the sensors, as well as possible, uniformly over the 22 km aperture encompassed by the A and B rings of LASA. These data indicate that, when the aperture is thus constrained, most of the gain is obtained with 50 sensors and that very little improvement is obtained by using more sensors. The reason for this is that these sensors introduce primarily coherent noise.

Figures 11A and 11B show how the gain using FS on unprefiltered traces varies as sensors are removed from the inner and outer rings of the subarray, respectively. It is seen that the gain drops uniformly as sensors are removed from the inner rings of the subarray, but that the gain stays very high as sensors are removed from the outer rings, and a large gain is obtained by using only the seven sensors in the 1 and 2 rings of the subarray, corresponding to an aperture of only 1 km. The important conclusion is that much of the gain produced with FS is obtained by employing amplitude differences of the microseismic noise which exist in the central cluster of the subarray, i.e., the

1 and 2 rings. In other words, the noise in these closely located sensors tends to be identical except for amplitude differences which occur due to either local geological conditions or the different response of the electronic equipment at about 0.2 cps which is where the noise against which the processing works is concentrated, as we shall see in Section IV. This matter is discussed further in Section VI. The FS processing assumes that the event is the same in each sensor and tries to minimize the noise power by taking a linear combination of the outputs from the closely located sensors. This conclusion has been verified by beam pattern studies and by running FS with the sensors equalized according to noise power and observing that the gain drops sharply from 25 db to 15 db. Thus, much of the FS gain is obtained by taking advantage of amplitude differences of coherent noise and not, as might be supposed, by velocity filtering based on the relative moveout of the noise across the subarray. Although this manner of obtaining a large gain is quite good at frequencies from $0.2 - 0.5$ cps, the gain above 1 cps may be quite poor. This is because the noise in this band is usually incoherent and DS-type processing is close to optimum in this band leading to $\sqrt{N}$ -type of gains.

IV. SIGNAL-TO-NOISE RATIO GAIN VS FREQUENCY AND APERTURE

The manner in which the signal-to-noise ratio gain of FS varies with frequency for subarray processing, inside and outside of the fitting interval, is of considerable importance. The results for different kinds of prefiltering will be markedly different, not only because of the different velocity structure of the noise at different frequencies, but because of the widely different noise power level at different frequencies. Recall that the FS processing is specifically designed to minimize output power and will therefore use the available processing degrees of freedom preferentially at the frequencies of high noise level. Typical raw trace noise spectra are shown in Fig. 12. Some results on SNR gain vs frequency for FS on unprefiltered traces are shown in Fig. 13. It will be noted that the data outside the fitting interval do not differ significantly from those inside the fitting interval. FS, WDS, and DS are compared in the fitting interval in Fig. 14. From Figs. 13 and 14 the gain of both FS and WDS is seen to be quite high at about 0.2 cps, roughly 20 db for FS, decreases to only a few db in the signal band of 1 to 2 cps and then rises to about 12 db in the band of 2 to 5 cps. The gain of DS is high above 1 cps. WDS works almost as well as FS at the low frequencies because in this band the processing is exploiting amplitude differences, not velocity structure. It is quite unfortunate that the FS processing should yield such low gain in the signal band. The reason for this is the great predominance of the microseismic noise power at 0.2 cps, which tends to obscure the estimates of noise spectra at other frequencies when measured with 0.5 cps resolution, corresponding to the reciprocal of the length

of the 2-second filter employed. Two other events have been subjected to the same analysis with comparable results.

The corresponding results for traces which have been bandpass prefiltered are shown in Fig. 15. These data (which have been verified on one other event) show that the gain of FS tends to stay high (12 db) across the signal frequency band of $0.6 - 2.0$ cps and that the gain of FS is almost as good as that of DS at the higher frequencies. Similar results are given in Fig. 16 for traces which have been prefiltered by the notch filter. Comparable results were obtained on one other event. The notch filter effectively removes the large spectral peak of the noise at 0.2 cps, and has the advantage with respect to the bandpass filter of not distorting the signal too much. Thus, Fig. 16 indicates the gain that can be obtained with prefiltering that does not essentially distort the signal. These results indicate that the gain of FS is relatively high all across the frequency band and is quite good in the signal band of 1 to 2 cps, of the order of 12 to 13 db. The overall gain is about 16 db. It is important to observe the advantage of FS over WDS and DS over most of the frequency band.

Figure 17 shows the spectra for the case where the sensors are spread over a 22 km aperture and the traces are not prefiltered. This is typical of three events analyzed. In this case the three forms of processing yield almost the same results because the microseisms at 0.2 cps tend to be incoherent over such a wide aperture and, since this is the predominating noise, the FS and WDS processing try to maximize the gain by simply adding the traces unweighted in much the manner that DS does. The overall gain of FS is 1.5 db, 3 db, better than that of WDS, DS, respectively. Figure 18

gives the corresponding results on the one event analyzed with 25 traces prefiltered by the bandpass filter. It is seen that there is even less of a difference between the three forms of processing. The wideband gain of FS tends to be about 3 db better than DS and 2 db better than WDS. The corresponding results for traces which have been prefiltered by the notch filter is shown in Fig. 19. In this case FS is about 4 db better than DS and 3 db better than WDS. These results are summarized in the following Table, which shows gains relative to the prefiltered traces.

Aperture (km)	Type of Prefiltering	Gain of FS (db)	Gain of WDS (db)	Gain of DS (db)
7	None	18÷	9÷	3÷
7	Bandpass	12*	7*	6*
7	Notch	12	7	4
22	None	14.5	13	11.5
22	Bandpass	14	12	11
22	Notch	16	13	12

NS = 25, NIM = 2, NFP = 21, three-minute fitting interval.

* Compare Figure 8.

÷ Compare Figure 9.

SIGNAL-TO-NOISE RATIO GAINS OF FS, WDS, DS FOR VARIOUS APERTURES AND PREFILTERS

Some of the numbers were mentioned earlier in connection with Figs. 6 and 7 which presented averages over many events.

The manner in which the signal-to-noise ratio gain varies with frequency for 25 sensors spread over 7, 15, 22 km apertures is shown in Fig. 20 for bandpass prefiltered traces. This graph indicates that for this prefiltering condition the results for FS for a 15 km aperture are roughly comparable to those of a 22 km aperture.

It is also possible to perform maximum-likelihood filtering of the individual maximum-likelihood outputs of the various subarrays. Figure 21 gives the gain vs frequency when four traces from a given ring of LASA are combined in this manner. It is seen that the curves tend to vary about a value of 6 db which is the gain one would obtain from four traces which contain independent noise. On the same event the gains of DS and WDS are also about 6 db when these forms of processing are applied to four FS traces. These results indicate that the combining of the FS outputs of subarrays can be done equally well by FS, WDS, DS. This was also seen to be the case in discussing Figs. 6 and 7.

V. DISTORTION OF FIRST MOTION

As was mentioned earlier, the use of nonrealizable filters (response before excitation) can produce false precursors. The maximum-likelihood synthesis procedure[5] forces the 25 filter impulse responses to sum to an impulse at zero delay, and thus no false precursor should be produced so long as the time-shifted signal waveforms are all identical for a time equal to the filter response duration [.05 sec × NIM × (NFP-1) = 2.0 sec]. However, in practice, seismometer to seismometer differences in signal for the first 2.0 sec do exist, and the possibility that the first motion of the filtered sum seismogram trace is false must be considered.

Figure 22A shows an example in which one whole cycle of artificial first motion results from signal differences. This was seen to disappear when the trace signal amplitudes were equalized, or when the same data were processed with a realizable filter. Since there is a substantial SNR loss in using a realizable filter (Fig. 2A), it was preferred that equalization be carried out on signal amplitude when using maximum-likelihood processing to enhance first motion.

A simulation was carried out to determine the amounts of amplitude and delay mismatch required to produce the precursor shown in Fig. 22A. First an artificial FS trace was generated using the same set of weights that gave the FS trace of Fig. 22A. The simulated input signals were sine waves with adjustable amplitude variations and shifts in arrival time. The signal amplitudes and arrival times were than measured on the actual data, and the artificial FS trace shown in Fig. 23A was generated using the measured values. The measured amplitude values scattered over a 2:1 range, and the

time delays were found to be in error by less than one sampling interval, 1/20 second. Figure 23A shows a precursor very similar to that of Fig. 22A. Figure 23B shows an artificial seismogram generated with only the actual arrival time shift errors included, and Fig. 23C shows an artificial seismogram with only the actual amplitude differences taken into account. It can be concluded that the precursor was predominantly a result of the amplitude differences.

A second maximum-likelihood run on the actual event was then made to see if the precursor could be removed by equalizing the input trace signal amplitudes. The result of this run is shown in Fig. 22B. The precursor is not visible on the FS trace. A third maximum-likelihood run on the event was made with a 21-point realizable filter. The FS trace is shown in Fig. 22C. No precursor was generated but only 14 db of noise reduction was achieved, compared to 24 db for the conditions of Fig. 22A and 20 db for Fig. 22B.

From this data we conclude that gain equalization on signal amplitudes allows control of the precursor without resort to the use of realizable filters which produce excessive loss in SNR gain. The amplitude corrections may be applied in two ways. For many P-phases on which there is a low enough noise level so that there is any chance of seeing first motion, the amplitudes can be picked well enough by eye. The alternative is to use the amplitude coefficients observed earlier from a strong event from the same epicentral region. From a nuclear test series and an earthquake aftershock series we have verified the repeatability of these coefficients for fixed epicenter, and experiments are now underway to evaluate how rapidly the coefficients change with epicenter shift.

VI. EXPLOITATION OF NOISE POWER INEQUALITIES AND WAVE NUMBER STRUCTURE BY OPTIMUM PROCESSORS

It has become quite popular to characterize microseismic noise in a three dimensional frequency-wave number space[8] and to describe linear seismic array processors by their gain as a function of frequency and wave number.[9,10] Such a description yields a relatively simple and esthetically pleasing explanation of the behavior of linear array processors. Because of this we are expending some effort in an attempt to relate frequency-wave number gains of optimum processors to the structure of microseismic noise in that same space. The detailed results will be reported elsewhere. Meanwhile, it has been determined that such a characterization of optimum filtering reveals only a part of the filter operation.

Frequency-wave number characterization assumes that the noise is space stationary. This includes the assumption that the noise power level at any frequency is independent of the position at which it is measured, an assumption which turns out not to be satisfied even when only the seismometers within a single subarray are considered. The differences cannot be accounted for by the consideration of local cultural and other surface noise in the area of the seismometers. It is not simply a matter of the differential degree of coupling to the earth of the different sensors either, since equalizing the gains on one teleseism neither equalizes the noise levels nor equalizes gains on some other teleseism from another place.

Some experiments have been carried out to indicate what effect these noise power differences can have upon optimum processors. These experiments help to indicate how much of the noise reduction obtained by optimum processing cannot be

accounted for by the array gain characteristic in frequency-wave number space. The following table gives some conditions under which a three-minute fitting interval preceding an event on 11/11/65 was used to design optimum filters to reject the noise.

CONDITIONS	FS	WDS	DS
11/11/65 Rat Is. event Site AØ, NS = 25 Unfiltered	25	14	3
11/11/65 Rat Is. event Site AØ, NS = 25 Unfiltered Noise Power Equalized	15	7	3
11/11/65 Rat Is. event Site AØ, NS = 2 Seismometers B4, B6 Unfiltered	8	5	1

The unfiltered subarray yielded a wideband noise reduction of 25 db for FS inside the fitting interval. The channels in the subarray were then gain equalized to yield equal noise power at each seismometer in the fitting interval. Optimum processors designed using this gain-equalized noise yielded only 15 db of noise reduction in the fitting interval using FS. In this situation it appears that 10 db of the gain obtained with the original noise could be attributed to the effective use of amplitude differences. For WDS 7 of the 14 db are attributed to this. It should be pointed out that the differences in power levels which accounted for the loss of gain when channels were

equalized were not strikingly large. If the average noise power of the channels was normalized to unity, then the largest and smallest channel r.m.s. noise levels were 1.35 and 0.60 before equalization.

A simple analysis of optimum weighted delay-and-sum processing for a two channel situation is of considerable assistance in trying to understand the extent to which the processors can use amplitude effects to achieve noise reduction. Suppose that

$$R = \begin{bmatrix} \sigma_1^2 & \rho\sigma_1\sigma_2 \\ \rho\sigma_1\sigma_2 & \sigma_2^2 \end{bmatrix}$$

is the measured zero lag correlation matrix of the two channels. It is not difficult to show that

$$\sigma^2 = \frac{(1-\rho^2)\,\sigma_1^2\,\sigma_2^2}{\sigma_1^2 + \sigma_2^2 - 2\rho\sigma_1\sigma_2}$$

is the minimum variance one can achieve by one-point filtering (WDS). Figure 24 shows some plots of the noise power obtainable as a function of correlation coefficient, ρ. One can see from those plots that if ρ is large, the extra noise reduction which can be obtained when $\sigma_1 \neq \sigma_2$ is considerable. One case plotted, $\sigma_1 = \sqrt{3}\ \sigma_2$, is approximately that measured for a two seismometer test case listed in the table. The correlation coefficient ρ for those seismometers was measured to be .905.

It is not difficult to see how gain can be achieved when correlation coefficients are large and positive. In the asymptotic case when $\rho = 1.0$ there is a weighted sum of the two channels which will yield zero output power. If the power levels in the two channels are not equal, then the sum of these two weights in the two-channel case will not be zero. These weights need simply to be multiplied by a constant to satisfy the maximum-likelihood constraint, namely that they sum to unity. The output power will remain at zero.

The effects of variations of signal amplitudes across a subarray upon processed signals were discussed in Section V of this report. This section has treated only the effects of variation in the noise which is used to design optimum filters.

Despite the large effect upon optimum processing of the differences in noise power at different seismometers it has still been possible in some cases to relate the gain characteristics of synthesized FS filters or WDS weights to the structure of noise in frequency-wave number space. A section of noise measured on 2/4/66 was pre-filtered with a 0.6 to 2.0 cps bandpass filter and optimum FS processing designed for subarray A0 using a three-minute fitting interval. The three-dimensional frequency wave-number Fourier transform of the impulse response of the subarray was computed.[11] At each frequency the noise power in each channel was normalized to unity and estimates of the wave number structure of the noise obtained. The method used to do this was equivalent to applying very narrow band filters to each seismometer, forming variously directed beams, and recording the percent of average power which appeared in each beam.

Figure 25 shows some of the gains in frequency-wave number space which were obtained by FS for a subarray. The location of the only significant noise concentration seen by subarray beams is indicated as well as the location of the signal which the subarray was designed to pass with no distortion. The organized noise at both frequencies appeared to be predominantly high velocity noise. At 0.6 and 1.0 cps the power in this spectral peak of organized noise had 0.5 and 0.35 as much power, respectively, as the average power of individual seismometers. The gains are unity at the location of the signal in wave number space. The tendency of the gain at both frequencies is to be low in the region of the greatest amount of organized noise. The gain becomes even greater than unity in some areas to achieve low values in the regions of high noise power.

Filter-and-sum (FS) processing was also designed for a collection of 25 seismometers spread over a 22 km aperture. Figure 26 shows part of the resulting gain characteristic in frequency-wave number space. Comments made in the case of the subarray are again valid.

In spite of the association of gain and power density in frequency-wave number space, the amplitude effects, not adequately characterized in such a coordinate system, cannot be overemphasized. Even when some relation between gain and power density can be found, it inevitably is true that the predicted noise reduction is considerably less than that actually obtained. The use which optimum processors make of the lack of spatial stationarity of the noise must be taken into account to adequately understand the processors.

VII. PROCESSING OF LONG-PERIOD DATA FROM THE EXTENDED ARRAY AT TFO

A number of events were processed from the extended array at TFSO (Tonto Forest Seismological Observatory) in order to determine the effectiveness of maximum-likelihood processing on long-period surface waves, about 20 second period. The data were obtained from digital recordings that included a triad of long-period vertical and horizontal instruments at TFSO itself plus similar triads at the mobile LRSM (Long Range Seismic Measurements) stations that were used to extend the TFSO aperture to 300 km. The long-period surface waves were aligned by picking the delays to match the theoretical delays as much as possible. The theoretical delays were obtained on the basis of a plane wave propagating across the array at a speed of about 3 km/sec. There was generally very poor agreement between the picked delays and the theoretical delays with errors of as much as 20%. Due to the long delay requirements, typically about 10 to 50 seconds, corresponding to 200 to 1000 sample values, only five channels could be combined at any time. A later version of the maximum-likelihood program will allow up to 25 channels to be combined. The events processed are given in the following table.

DATE	REGION	TYPE OF INSTRUMENT
6/11/65	Easter Island	Long-Period Vertical
6/11/65	Rat Island	Long-Period Vertical
6/24/65	Guererro, Mexico	Long-Period Horizontal
6/24/65	Guererro, Mexico	Long-Period Vertical

It was found that most of the noise preceding the long-period surface waves was due to instrument or telemetry instabilities. The processing used a NIM of 22, that is, the data was decimated to use one sample value every 1.1 sec. We used NFP = 11, so that the filter impulse responses were 11.0 seconds long, and a three-minute fitting interval. The gains of FS, WDS, DS were quite similar, about 6 to 8 db, indicating that the noise was independent between sensors. There was little signal distortion noticeable in the processed traces relative to the raw-data traces. This is encouraging in view of the dispersion experienced by the long-period surface waves as they travel across the array. The results are shown in Fig. 27.

These results must be considered tentative until a better test can be made using the 21 sets of three-component long-period sensors now being installed at LASA.

VIII. EXAMPLES OF WEAK EVENT PROCESSING

A number of weak events were processed by FS, WDS, DS to determine if these events could be extracted from the background noise. One such event is the 12/11/65 Commander Islands event which was locatable from reports of several U. S. C. and G. S. worldwide stations and found to exist in our library of recorded tapes that were saved for analysis of other detected events. This event was invisible on LASA raw data traces. Its parameters, based on the fragmentatory C. and G. S. reports, are given in the following table along with those of a strong event of 1/16/66, in the same region.

12/11/65 Commander Islands Event

Origin Time: 03:39:47 ± 5
North Latitude: 55.°
East Longitude: 16.7°
Average LASA Magnitude: 3.5 (estimated)

1/16/66 Commander Islands Event

Origin Time: 19:44:39.5
North Latitude: 54.9°
East Longitude: 165.8°
Magnitude: 5.6
Depth: 15 km
Distance: 52.7°
Azimuth: 313.5°
Horizontal Velocity: 14.99 km/sec

The parameters of this latter event were used in the processing to obtain the azimuth and horizontal velocity of the 12/11/65 event.

All 21 subarrays were processed by FS, WDS, DS and 19 of these gave negative results which were similar to those given in Fig. 28A. However, the event was visible at sites C3 and D2 as indicated in Figs. 28B and 28C. In each of these latter three figures, the top trace corresponds to the 1Ø sensor of the subarray and then the next three traces are WDS, DS, FS, in that order. The results of stacking the two good subarrays are shown in Fig. 28D. It is seen that the event is quite complex which identifies it as a natural event and not a nuclear explosion. It is also observed that the event is not visible on the DS and WDS traces for subarray processing so that for unprefiltered processing of subarrays it would not have been possible to see the event without using FS processing.

The usual 0.6 to 2.0 cps bandpass prefiltering was used followed by DS, WDS, FS processing and it was not possible to see the event on any of the processed traces. The reason for this is that the event happened to be of rather high frequency, about 1.5 cps. Thus, when a different bandpass prefilter was used, 1.15 to 3.5 cps, it was possible to see the event on the DS, WDS, and FS processed traces of sites C3 and D2. The improvement was most spectacular for site C3. For site D2 the SNR was improved but the arrival time was somewhat obscured. The prefilter also was used to extract the signal from site B3 where it could not previously be found using either the 0.6 to 2.0 cps prefilter or no prefilter at all. The results for sites B3, C3, and D2 are shown in Figs. 29A, 29B and 29C, respectively. It is important to stress that there is no a priori way in which one knows how to choose the appropriate form of prefiltering. One method of determining the characteristics of an event is to use unprefiltered traces processed by FS.

Another weak event which was processed is the 10/1/65 Rat Island event whose parameters are given in the following table.

10/1/65 Rat Island Event

Origin Time: 12:53:48
North Latitude: 50.4°
East Longitude: 178.4°
Magnitude: 3.7 (U. S. C. & G. S.)
Average LASA Magnitude: 4.0 (estimated)
Depth: 33 km
Distance: 48.1°
Azimuth: 303.6°
Horizontal Velocity: 14.39 km/sec.

Figure 30 shows typical individual seismometer recordings from site B4 and the results of the WDS, DS, and FS processing. The event is barely visible on the FS processed trace and not visible on either WDS or DS. Figure 31 shows the FS processed traces from seven subarrays and the results of stacking these traces by WDS, DS, FS processing. The event is somewhat more visible after this processing. Thus, we have another example in which the FS processing is extremely valuable for the extraction of a weak event from noise.

IX. EFFECT OF SIGNAL AMPLITUDE SCATTER

Using a population of 18 events, a number of measurements have been made of the scatter of signal amplitude level within a subarray and between subarrays. It was found that within a subarray on an event with typical scatter, the r.m.s. deviation from the mean was 18%, and the extreme values differed by an average of 1.8:1. On an event with typical scatter among the subarrays (as deduced from "1Ø" seismometer traces) the r.m.s. scatter from the mean was ± 38% and the extremes differed by an average of 4:1. Thus the scatter between subarrays is significantly wider than that within one subarray, either on the basis of r.m.s. amplitude scatter or amplitude extremes. In fact, on several events having very large scatter, a 2.6:1 scatter within a subarray was associated with a 9:1 scatter over the array.

It was found that the set of amplitudes was different from event to event, unless the epicenters were coincident. How rapid the sets of amplitudes for two events decorrelate with distance between the two epicenters is not known yet, but the amplitudes are presumed to be less epicenter-sensitive over a subarray than over the entire array.

The variation of signal amplitudes within one subarray can have several consequences. The maximum-likelihood filter (FS) operates on the assumption that the signal, or event, in each sensor of the subarray is identical to that in every other sensor. If this is not the case, there can conceivably be a serious degradation in the performance of the maximum-likelihood filter. As an example, it is possible for the event to be weak in some sensors, and for the maximum-likelihood filter to weight these traces heavily, so that the processed traces will have a weak signal. This effect has

been noticed when attempting to process recordings that include traces from malfunctioning seismometers. However, as was mentioned in Section I, if an analyst examines the traces to be processed and deletes any which have an event which is smaller by about 6 db than the average of those traces which are to be processed, then we have found that the amount of signal amplitude loss in the final processed output trace relative to the delayed sum is rarely more than 1.5 to 2.0 db. The amplitudes can all be normalized by using visual amplitude picks or stored tables, as discussed in Section V. Either way the deleterious effects of amplitude scatter within a subarray are minor if properly guarded against.

When the availability of 21 subarrays is considered, the amplitude scatter constitutes a distinct asset. This is illustrated by the two event case histories described in the Section VIII. A number of events that would be missed on an average subarray or the poorest subarrays are detectable on one or more subarrays. Since these best subarrays are not the same subarrays from event to event, it follows that on certain events a system of 21 subarrays will be more sensitive than a system composed of just one (e.g. an array of the Vela observatory or UKAEA type) by the factor 4 (0.6 mag.) even if only the single best subarray is examined. This is particularly important when the station must provide coverage of a wide variety of epicenters; if only one epicentral region is to be monitored, careful siting of a small array will mitigate this inferiority somewhat.

When the 21 subarrays are properly combined, a further SNR gain is produced causing the SNR of the final output trace to exceed even that of the best trace. By

properly combined, we mean amplitude weighted in proportion to the individual voltage SNR and then added. This scheme ("Brennan combining") is optimum if the noises are independent. (WDS reduces to this for the equal signal case.) The question arises whether the $\sqrt{N}$ gain (over average subarray SNR) figures we have been quoting for DS subarray combining are inferior to what might be achieved taking into account the unequal signal amplitudes. This has been tested for 10 events and the SNR gain for DS was determined to average only 1.5 db less than that for Brennan combining.

We conclude that signal amplitude scatter constitutes one of the advantages of having both a large aperture and large number of subarrays. Deleterious effects of amplitude scatter can be corrected.

X. SUPPRESSION OF INTERFERING TELESEISMS

The ability of a LASA to reject unwanted teleseismic energy from specific source regions in favor of desired teleseisms is important for several purposes, for example, to maintain surveillance for nuclear test activity during a strong earthquake. In principle, the nulls in the directional response of LASA can be made very deep and therefore we have experimented with steering such nulls toward interfering teleseisms. Optimally the null should be steered over the signal bandwidth, which can be done using FS processing in either of two ways. Filters can be set up either on the basis of a calculated directional model of the wanted and unwanted teleseisms, or by actually placing in the fitting interval part of the unwanted event (or another event from the same place) while controlling the steering delays to point toward the wanted event.

A test of the second procedure was carried out using two phases of the same event to simulate the P phase from each of two events. The results are shown in Fig. 32. A 32 km end-fire linear array of LASA sensors was formed by selecting a particular 25 elements of the LASA. The unwanted event is P from Long Shot and the role of the wanted event is played by the PcP phase from the same event. The three-minute fitting interval ended part way through the P coda, but before PcP. This PcP phase acts like another teleseism from the same bearing as P, but at a widely different distance. PcP arrived at a horizontal phase velocity different from that of P, that corresponded to a shift of beam position amounting to 1.8 times the 3 db DS beamwidth of the 32 km linear array.

Note that the suppression of P relative to PcP is quite marked, and this is particularly true with FS which allows the nulling out of P to be frequency dependent. Total suppression of P was 32 db using FS on just the 25 seismometers and 32 km aperture.

XI. CONCLUSIONS

It has been determined that prefiltering of data before designing and applying FS or WDS processors has a considerable effect upon the gain of the processors as a function of frequency. If truly wideband signals or signals in the band 0.1 to 0.5 cps are of interest, then unfiltered FS processing is to be recommended. If some minor distortion is allowed but first motion is to be preserved, then a notch prefilter, designed to reject low frequency microseisms , can be used. Prefiltering with a 0.6 to 2.0 cps bandpass filter is recommended if first motion can be distorted and only more gross characteristics of the waveform, such as complexity, are under consideration.

If we include the case when data are not prefiltered, then it has been shown that increasing the subarray size from 7 km to about 15 to 20 km, and spreading seismometers uniformly over the aperture, does not reduce the SNR gains achievable. In fact, for prefiltered data SNR gains almost comparable to those for FS applied to a 7 km subarray can be obtained using DS or WDS processing. The FS gains for prefiltered data and the larger aperture are as good or better than those for prefiltered 7 km subarrays. This important result would mitigate in favor of a larger size subarray with the 25 sensors spread uniformly over the aperture. The uniform spacing (minimum separation greater than 2 km) is recommended since closer spacing would require the application of FS processing to achieve significant SNR gains. The fraction of events requiring FS processing should be smaller for the larger subarrays than for the 7 km subarrays.

The use of FS processing on-line or on-site in a large subarray certainly seems unjustified in view of the great cost of installing the necessary computing equipment. However, the 3 to 4 db advantage of FS still makes it desirable as an off-line processing method, where the computing equipment is readily available, and it is desired to obtain as much gain as possible to identify weak events.

In summary, the subarray aperture should be increased to 15 to 20 km and on-line processing should consist of prefiltering, either bandpass or notch, followed by DS. Further SNR gains can be achieved off-line by using appropriate prefiltering followed by FS, WDS, or even DS, depending upon the availability of computing equipment. Special situations such as the almost simultaneous arrival of two teleseisms should also be handled off-line using techniques which are suitable for the purpose.

Signal amplitude variations as large as 9:1 between subarrays mean that some small number of subarrays, the particular ones depending upon the event epicenter, may have considerably better SNR than others. This can be of considerable value for small events. It should also be mentioned that if FS processing is to be done off-line then it is highly desirable to have amplitude station corrections. These corrections would have to be inserted for various bearing and epicentral distances. They are required to reduce to a minimum the precursors and other signal distortions which may be introduced by FS processing.

REFERENCES

1. P. E. Green, Jr., et al, "Principles of an Experimental Large Aperture Seismic Array (LASA)," Proc. I. E. E. E., December 1965, pp. 1821-1833.

2. C. B. Forbes, et al, "The LASA Sensing System Design, Installation, and Operation," Proc. I. E. E. E., December 1965, pp. 1834-1843.

3. R. V. Wood, Jr., et al, "Large Aperture Seismic Array Signal Handling System," Proc. I. E. E. E., December 1965, pp. 1844-1851.

4. H. W. Briscoe and P. L. Fleck, "Data Recording and Processing for the Experimental Large Aperture Seismic Array," Proc. I. E. E. E., December 1965, pp. 1852-1859.

5. J. Capon, et al, "A Frequency-Domain Synthesis Procedure for Multidimensional Maximum-Likelihood Processing of Seismic Arrays," M.I.T., Lincoln Laboratory Technical Note 1966-29, 6 May 1966.

6. E. J. Kelly, "LASA On-Line Detection, Location and Signal-to-Noise Enhancement," M.I.T., Lincoln Laboratory Technical Note 1966-36, July 1966.

7. H. W. Briscoe and R. M. Sheppard, "A Study of the Capability of a LASA to Aid the Identification of a Seismic Source," M.I.T., Lincoln Laboratory Technical Note 1966-38, July 1966.

8. E. J. Kelly, "The Representation of Seismic Waves in Frequency-Wave Number Space," M.I.T., Lincoln Laboratory Group Report 1964-15, 6 March 1964.

9. J. P. Burg, "Three-Dimensional Filtering with an Array of Seismometers," Geophysics, XXIX, October 1964, pp. 693-713.

10. P. Embree, et al, "Wide-Band Velocity Filtering--The Pie Slice Process," Geophysics, XXVII, December 1963, pp. 948-974.

11. R. T. Lacoss, "Geometry and Patterns of Large Aperture Seismic Arrays," M.I.T., Lincoln Laboratory Technical Note 1965-64, 31 December 1965.

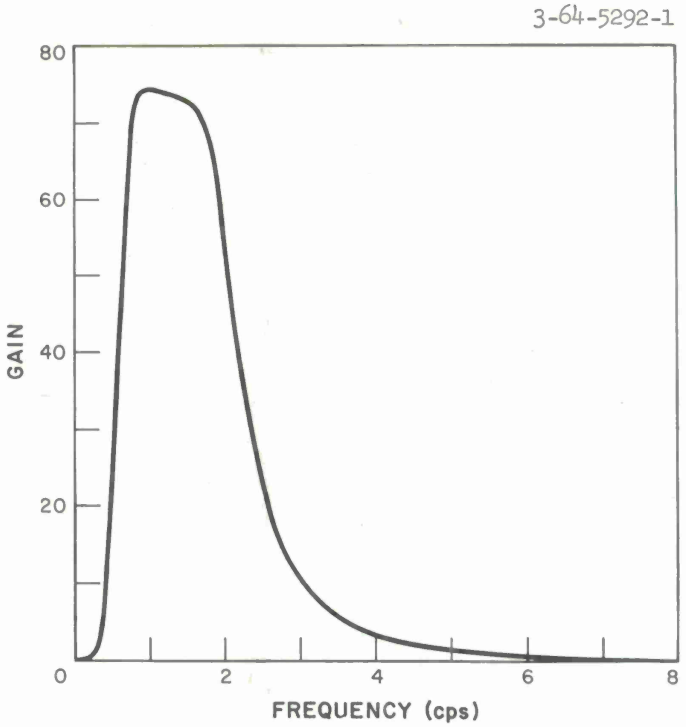

Figure 1(a). Frequency Response of the Bandpass Filter.

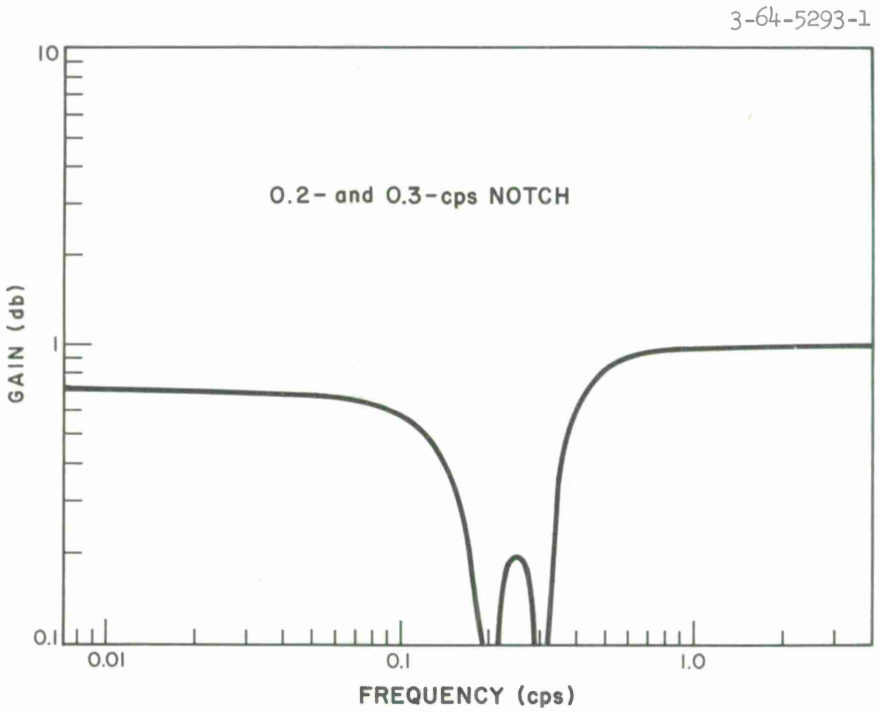

Figure 1(b). Frequency Response of Notch Filter.

3-DO-3068(1)

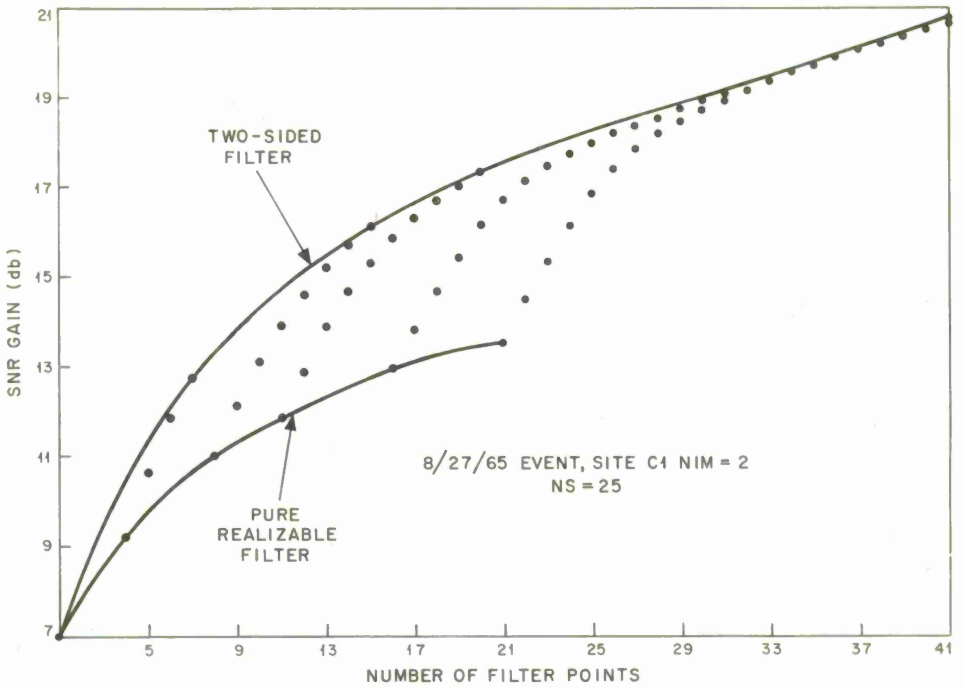

Figure 2(a). Signal-to-Noise Ratio Gain of Maximum-Likelihood Filter versus Number of Filter Points for Unprefiltered Traces.

3-64-5317

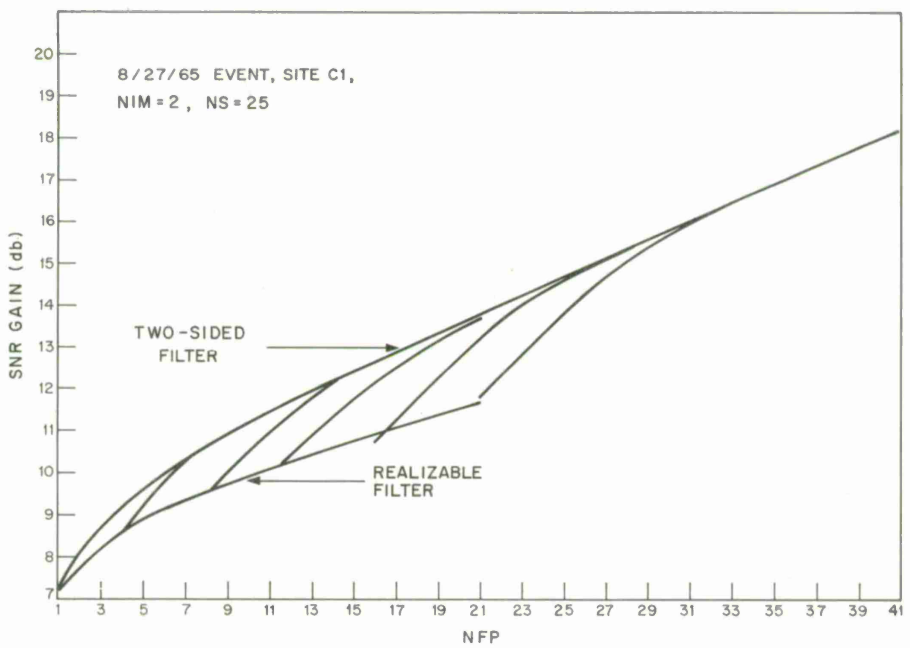

Figure 2(b). Signal-to-Noise Ratio Gain of Maximum-Likelihood Filter versus Number of Filter Points for Bandpass Prefiltered Traces.

3-64-4983

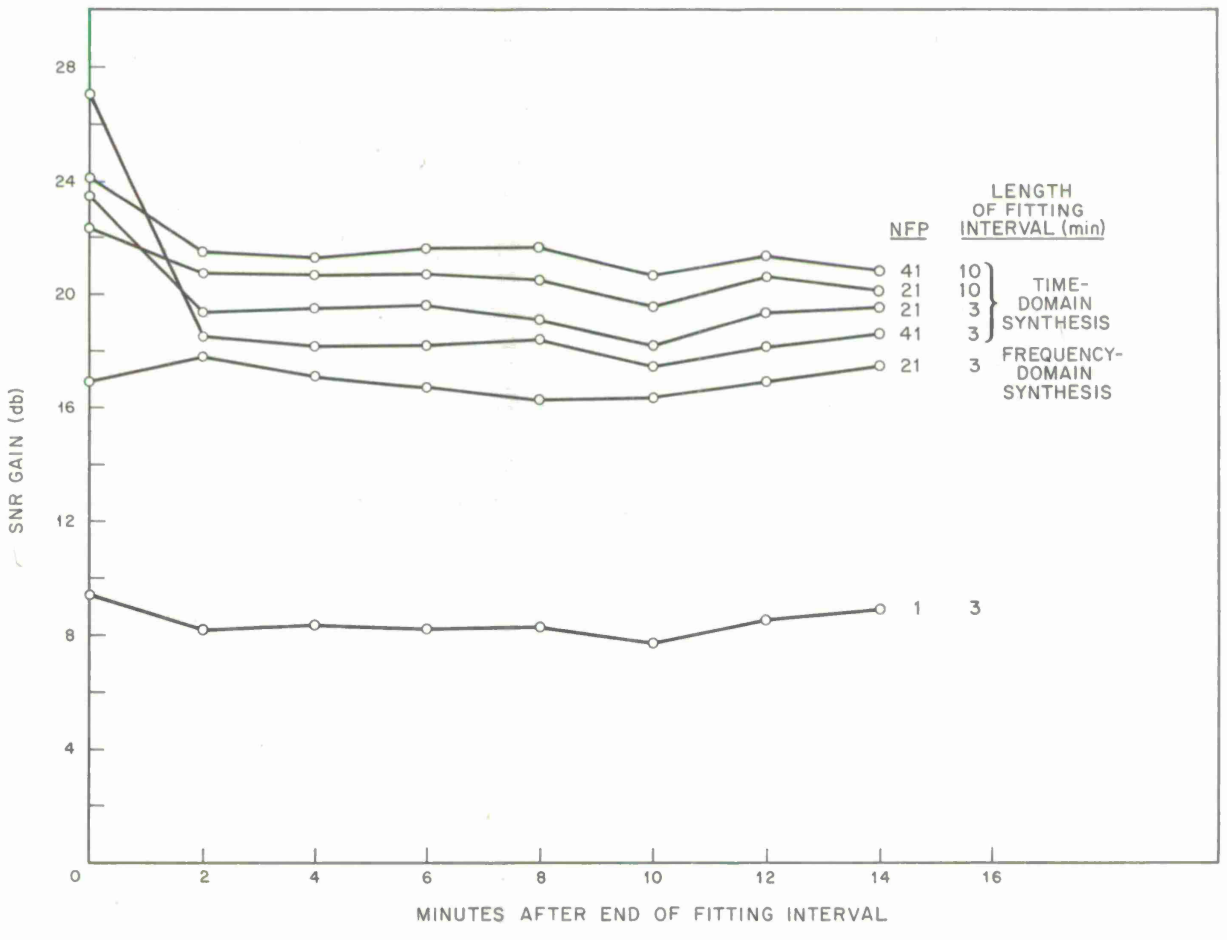

Figure 3. Signal-to-Noise Ratio Gain of Maximum-Likelihood Filter Outside the Fitting Interval for Various NFP and Fitting Interval Lengths.

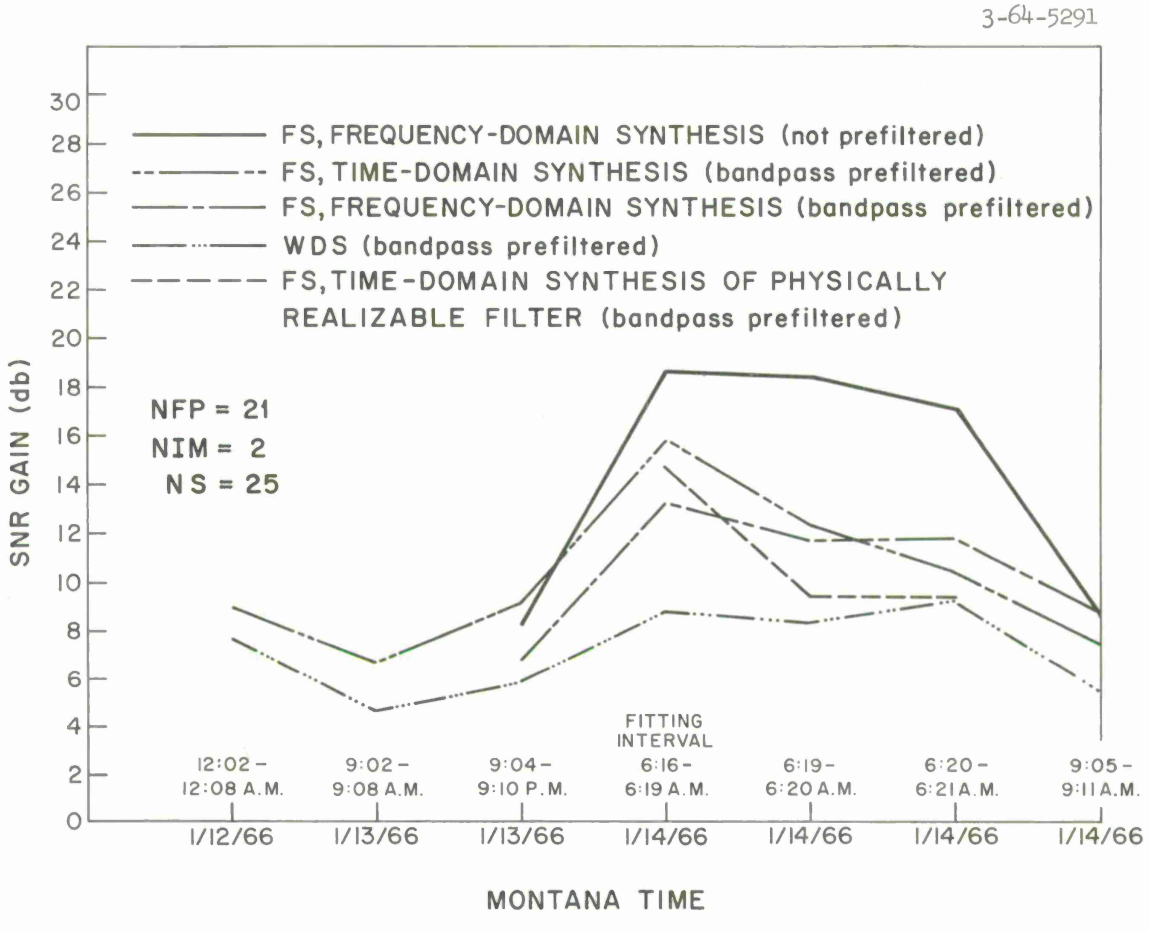

Figure 4. Signal-to-Noise Ratio Gain of Maximum-Likelihood Filter for Minutes, Hours, and Days After the Fitting Interval.

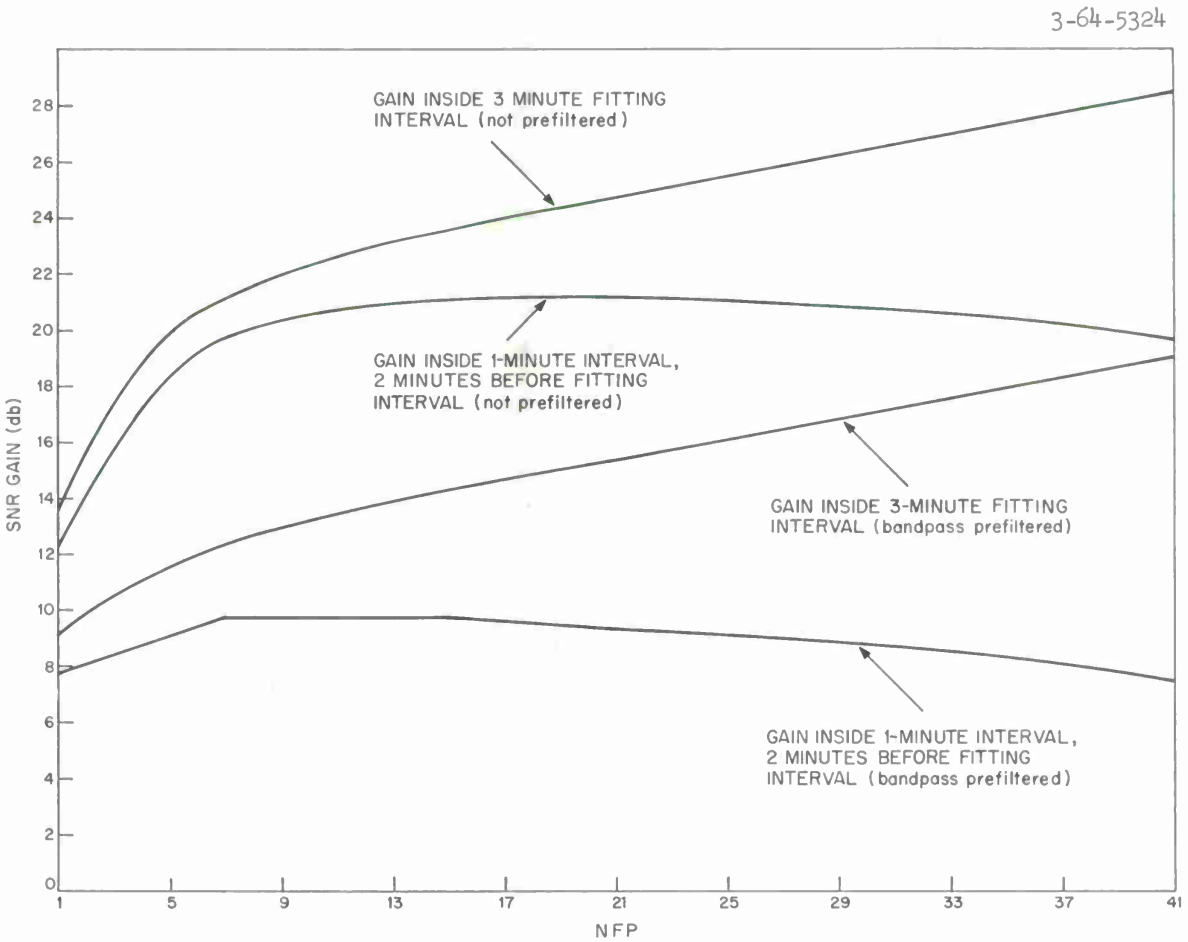

Figure 5. Signal-to-Noise Ratio Gain of Maximum-Likelihood Filter versus NFP Inside and Outside the Fitting Interval for Unprefiltered and Bandpass Prefiltered Traces.

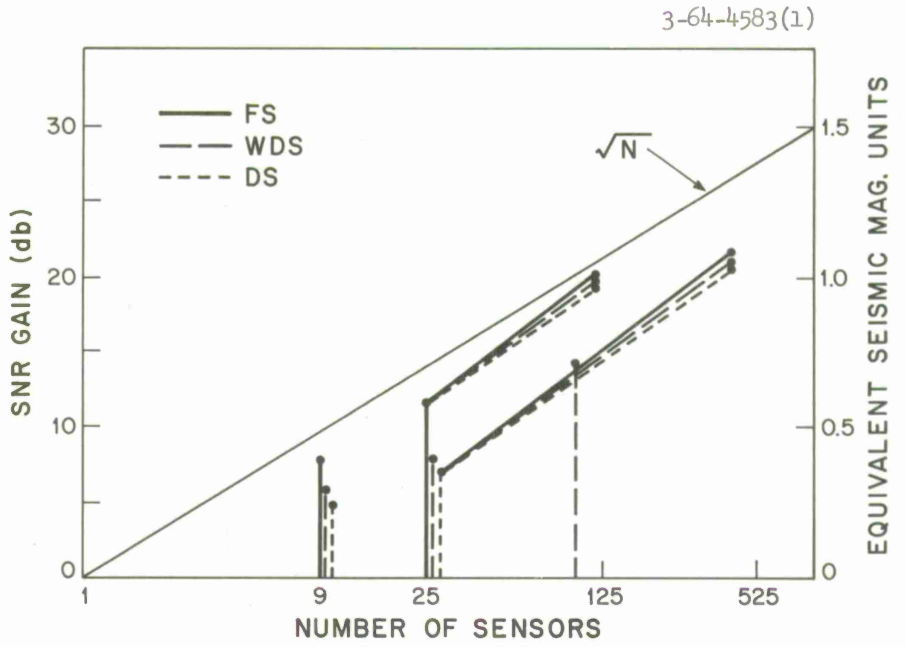

Figure 6. Signal-to-Noise Ratio Gain of Various Forms of Processing versus Number of Sensors for Bandpass Prefiltered Traces.

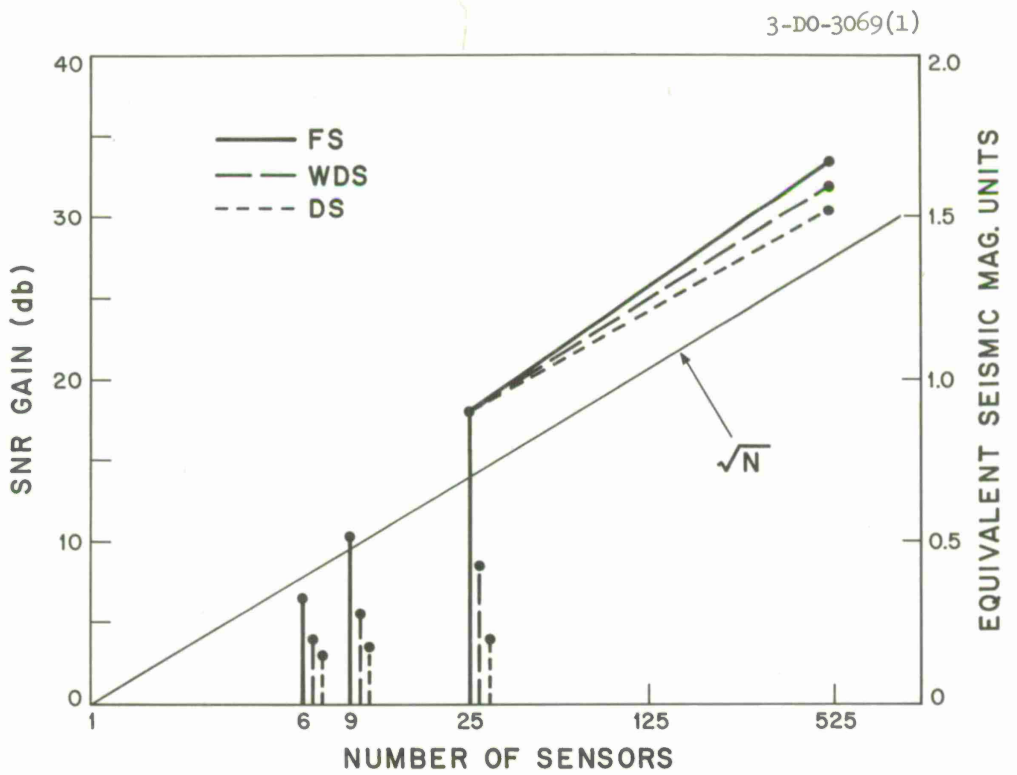

Figure 7. Signal-to-Noise Ratio Gain of Various Forms of Processing versus Number of Sensors for Unprefiltered Traces.

3-64-4584(1)

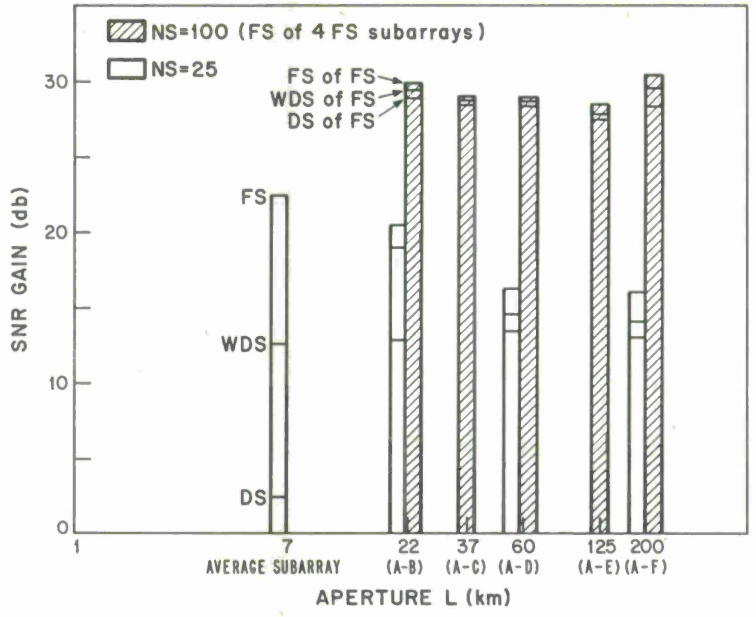

Figure 8. Signal-to-Noise Ratio Gain of Various Forms of Processing versus Aperture.

3-64-5325

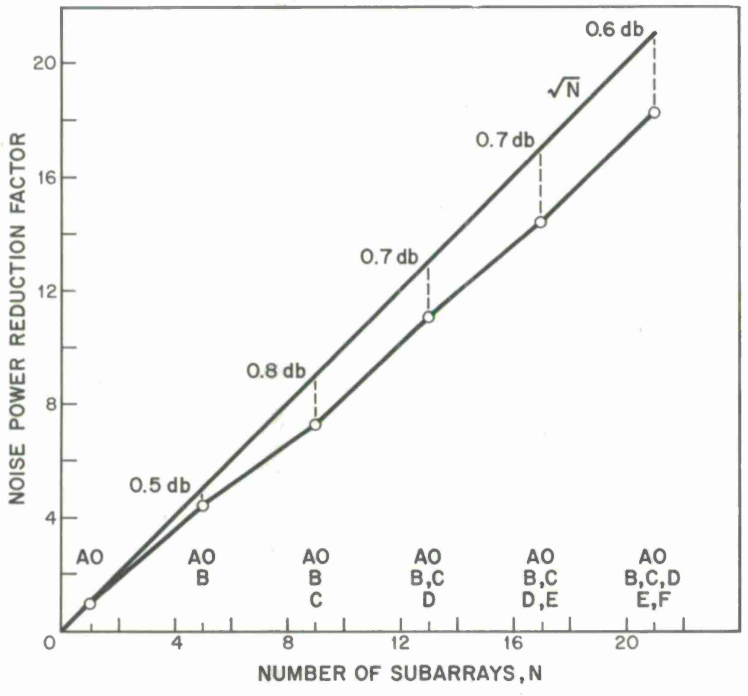

Figure 9. Signal-to-Noise Ratio Gain of Delayed Sum of Straight Sum Subarray Outputs versus Aperture.

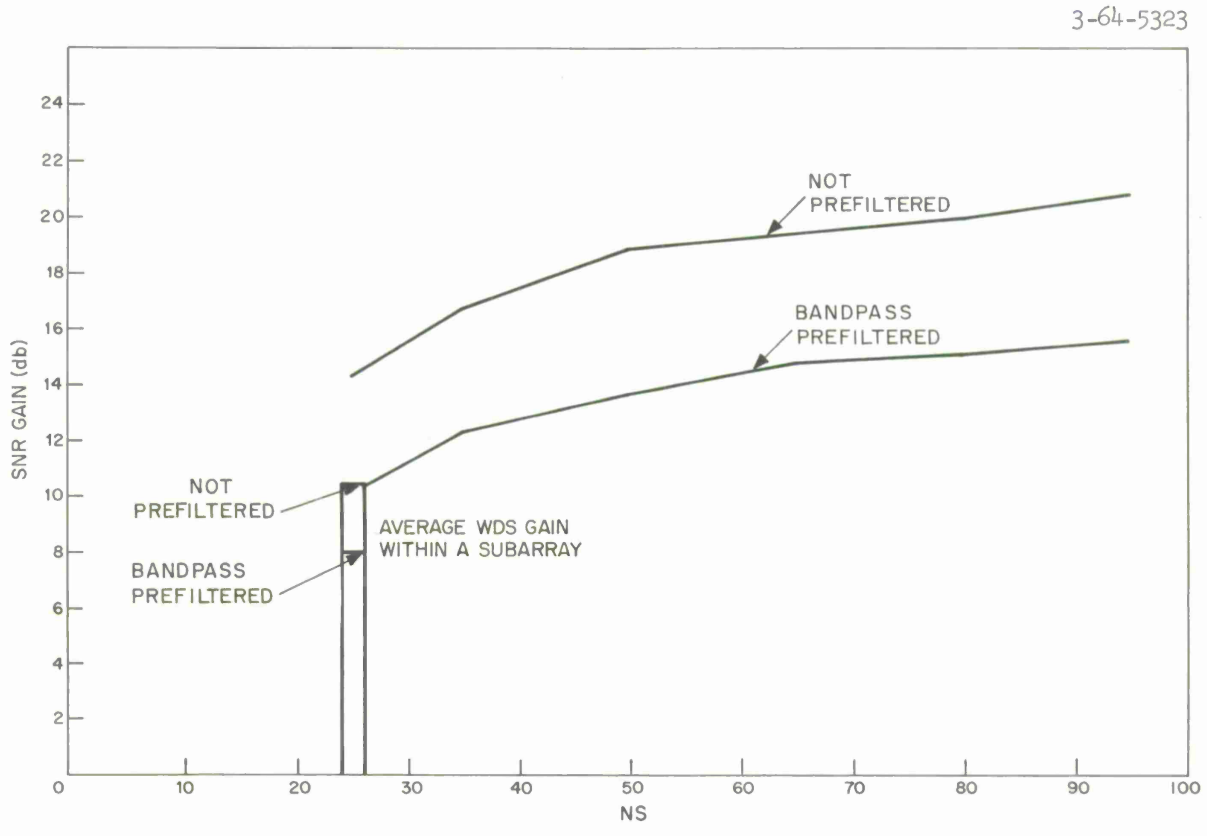

Figure 10. Signal-to-Noise Ratio Gain of Weighted Delay-and-Sum Versus Number of Sensors, Sensors Within A and B rings of LASA.

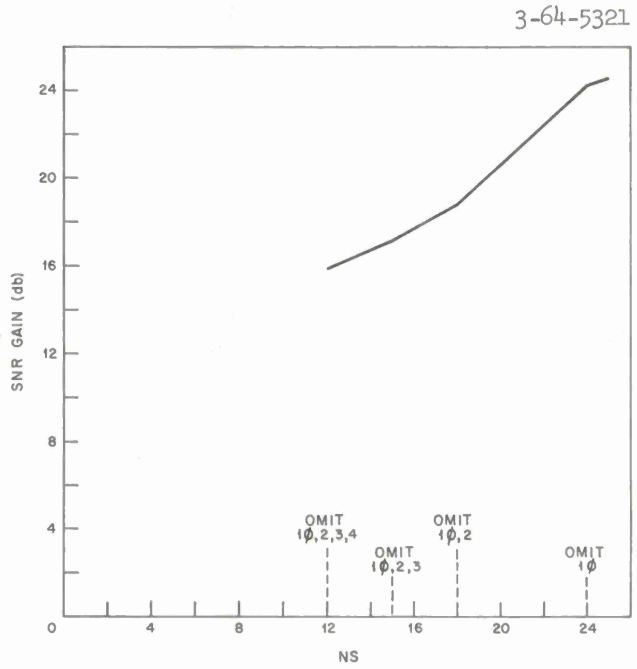

Figure 11(a). Signal-to-Noise Ratio Gain of Maximum-Likelihood Filter versus Number of Sensors, Sensors Removed from Inside Rings of Subarrays.

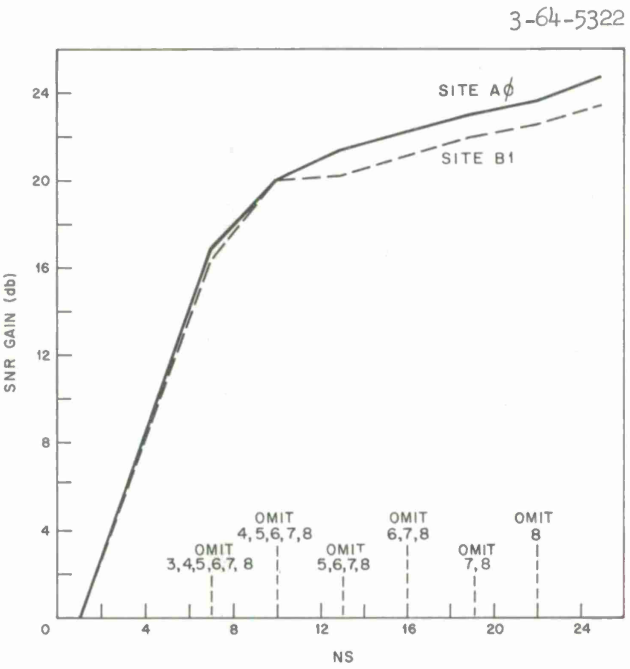

Figure 11(b). Signal-to-Noise Ratio Gain of Maximum-Likelihood Filter versus Number of Sensors, Sensors Removed from Outside Rings of Subarray.

3-64-5294

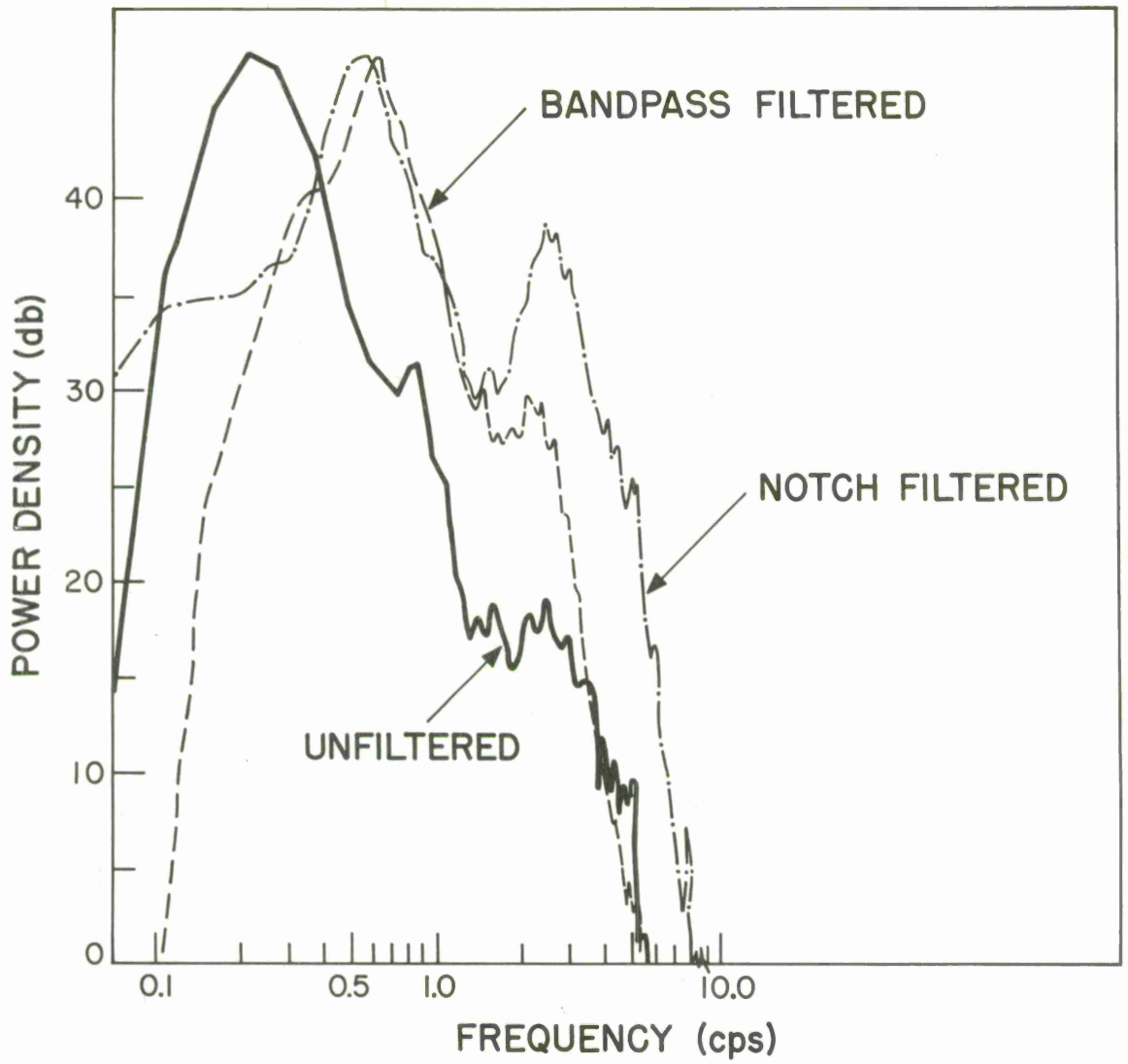

Figure 12. Typical Input Trace Noise Power Spectral Density.

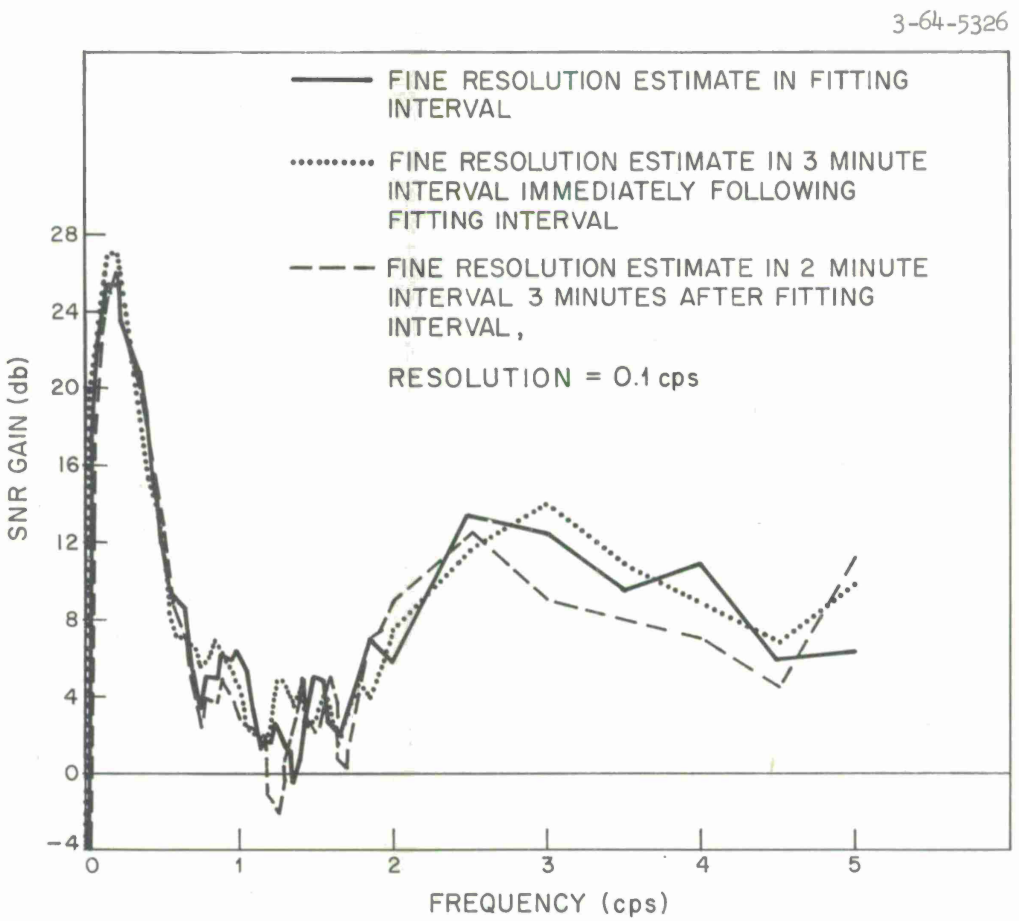

Figure 13. Signal-to-Noise Ratio Gain for 7 km Subarray versus Frequency, Inside and Outside of Fitting Interval for Frequency-Domain Maximum-Likelihood Filter.

3-64-5195-1

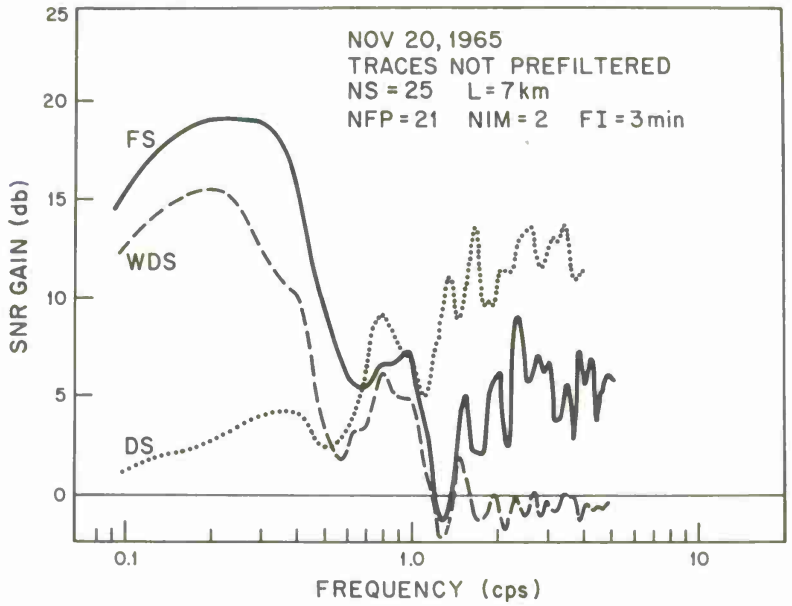

Figure 14. Signal-to-Noise Ratio Gain of FS, WDS, DS for 7 km Subarray versus Frequency, Input Traces Not Prefiltered.

3-64-5229-1

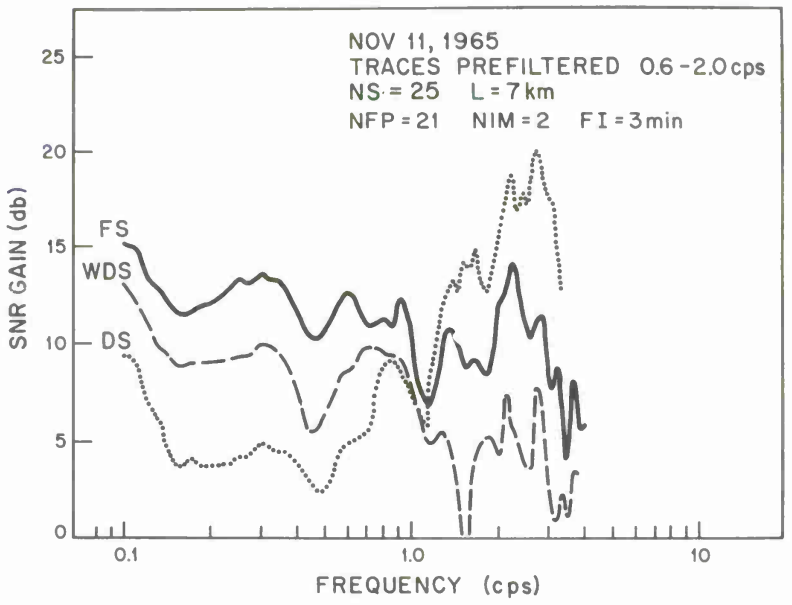

Figure 15. Signal-to-Noise Ratio Gain of FS, WDS, DS for 7 km Subarray versus Frequency, Input Traces Bandpass Prefiltered.

3-64-5231-1

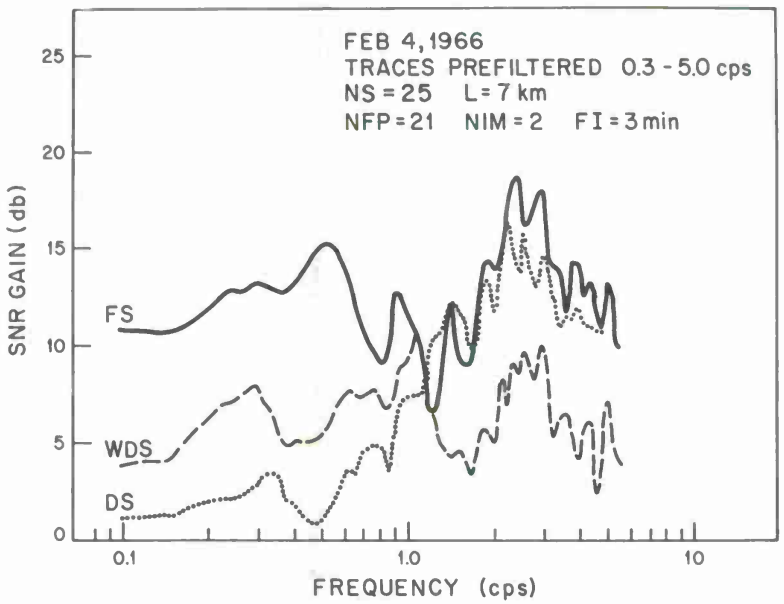

Figure 16. Signal-to-Noise Ratio Gain of FS, WDS, DS for 7 km Subarray versus Frequency, Input Traces Notch Prefiltered.

3-64-5235-1

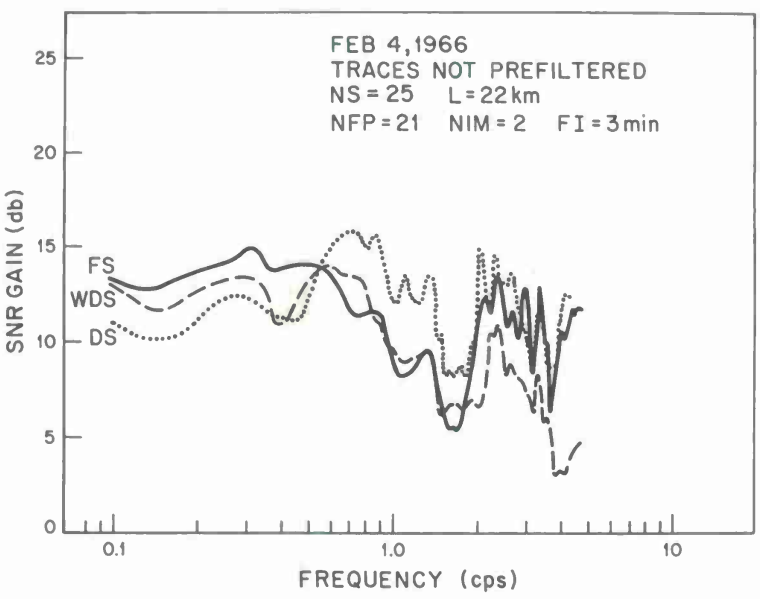

Figure 17. Signal-to-Noise Ratio Gain of FS, WDS, DS versus Frequency, 25 Sensors Covering 22 km, Input Traces Not Prefiltered.

3-64-5230-1

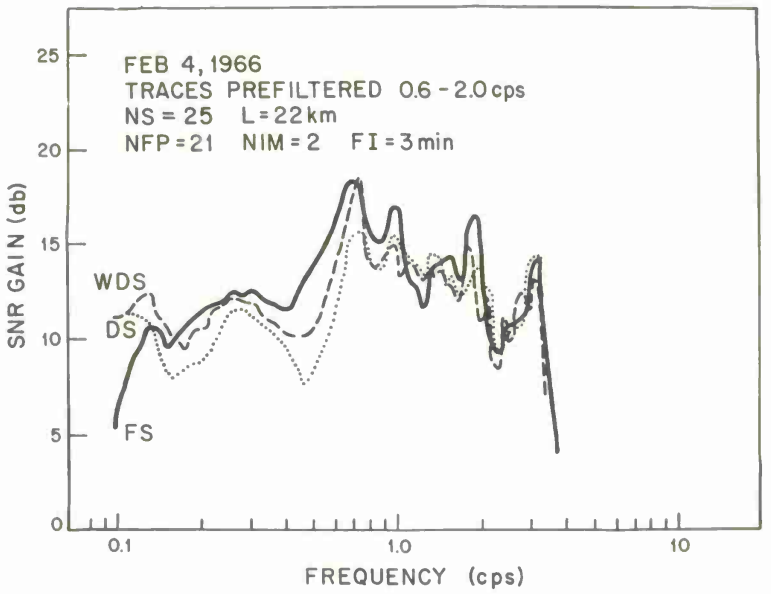

Figure 18. Signal-to-Noise Ratio Gain of FS, WDS, DS versus Frequency, 25 Sensors Covering 22 km, Input Traces Bandpass Prefiltered.

3-64-5232-1

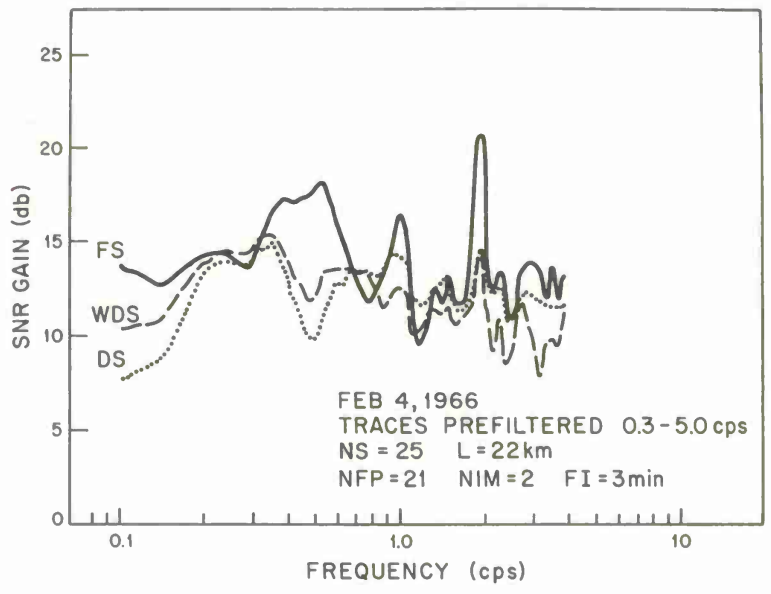

Figure 19. Signal-to-Noise Ratio Gain of FS, WDS, DS versus Frequency, 25 Sensors Covering 22 km, Input Traces Notch Prefiltered.

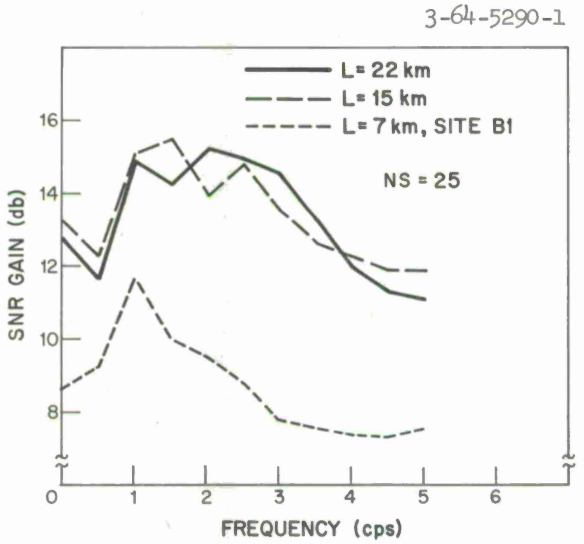

Figure 20. Signal-to-Noise Ratio Gain of Maximum-Likelihood Filter versus Frequency for 7, 15, 22 km Apertures, Corresponding to Subarray, AB, ABC rings of LASA, NS = 25, Input Traces Bandpass Prefiltered.

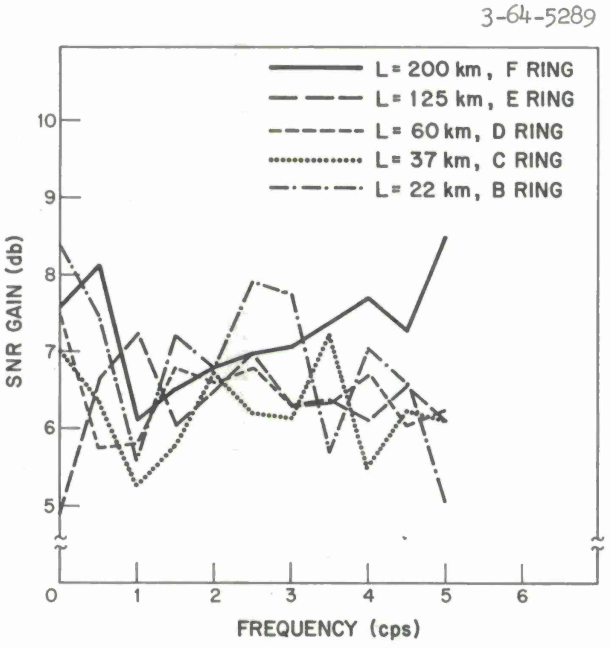

Figure 21. Signal-to-Noise Ratio Gain versus Frequency for FS Processing of Four FS Traces from Various Rings in LASA.

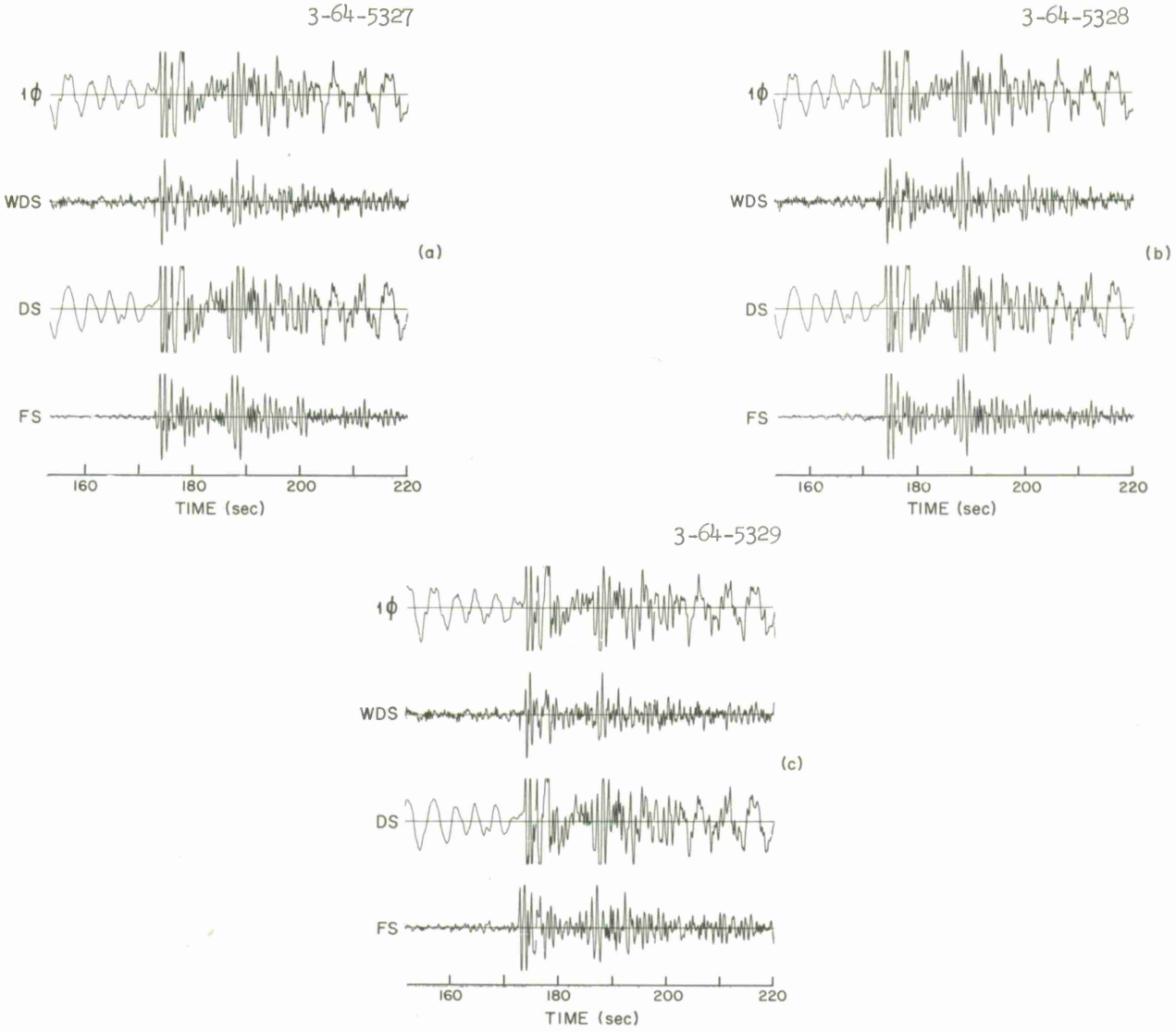

Figure 22(a). Precursor Introduced by Two-Sided FS Filter.

(b). Elimination of Precursor by Employing Signal Amplitude Gain Equalization.

(c). Results of FS Processing Using a 21-Point Physically Realizable Filter.

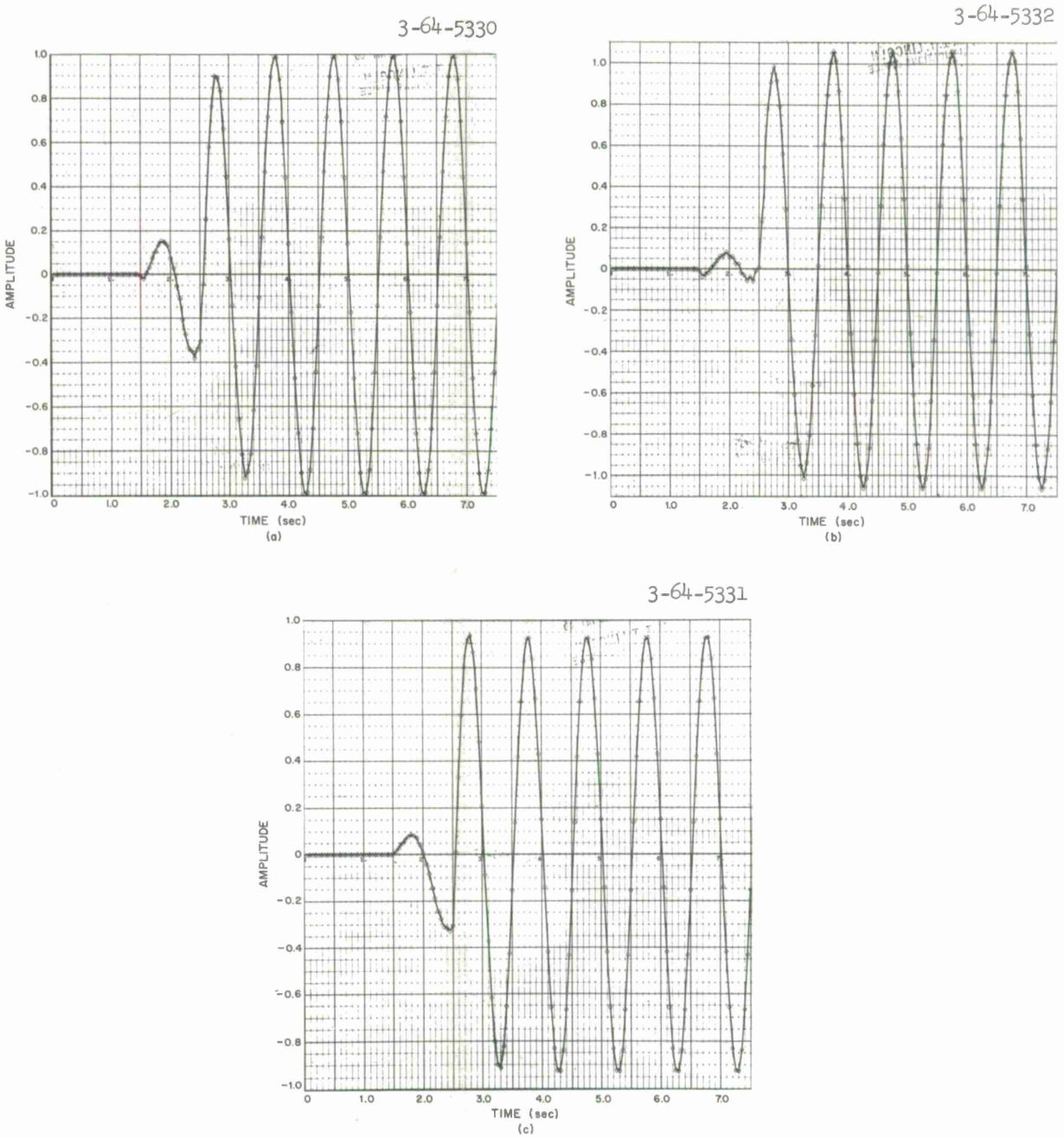

Figure 23(a). Artificial Seismogram Illustrating the Precursor Introduced by Two-Sided FS Filter due to Signal Amplitude Scatter and Timing Errors.

(b). Precursor Due to Timing Errors Alone.

(c). Precursor Due to Amplitude Scatter Alone.

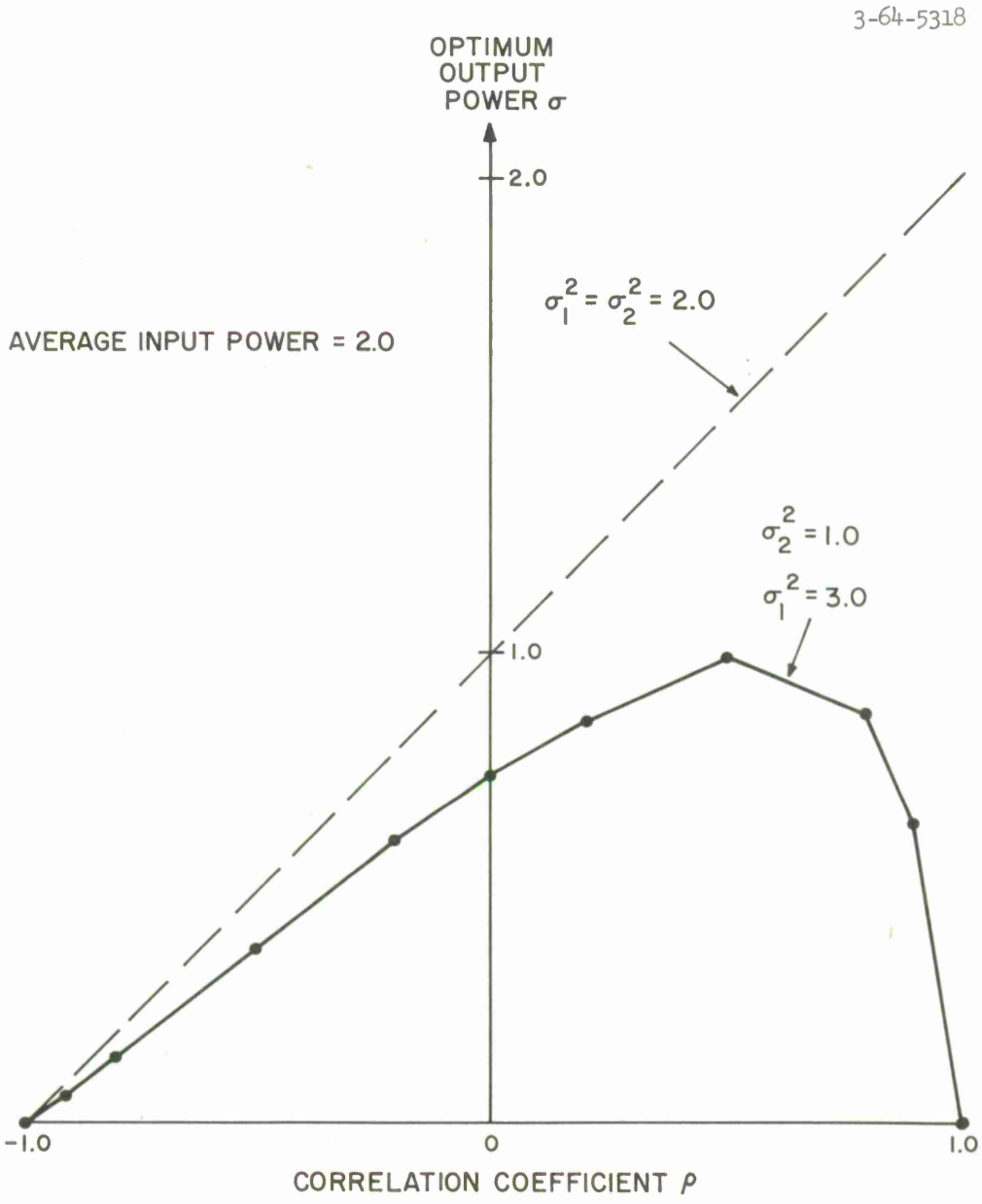

Figure 24. Optimum Noise Power Reduction Obtained from Two Seismometers Using One-Point Filters.

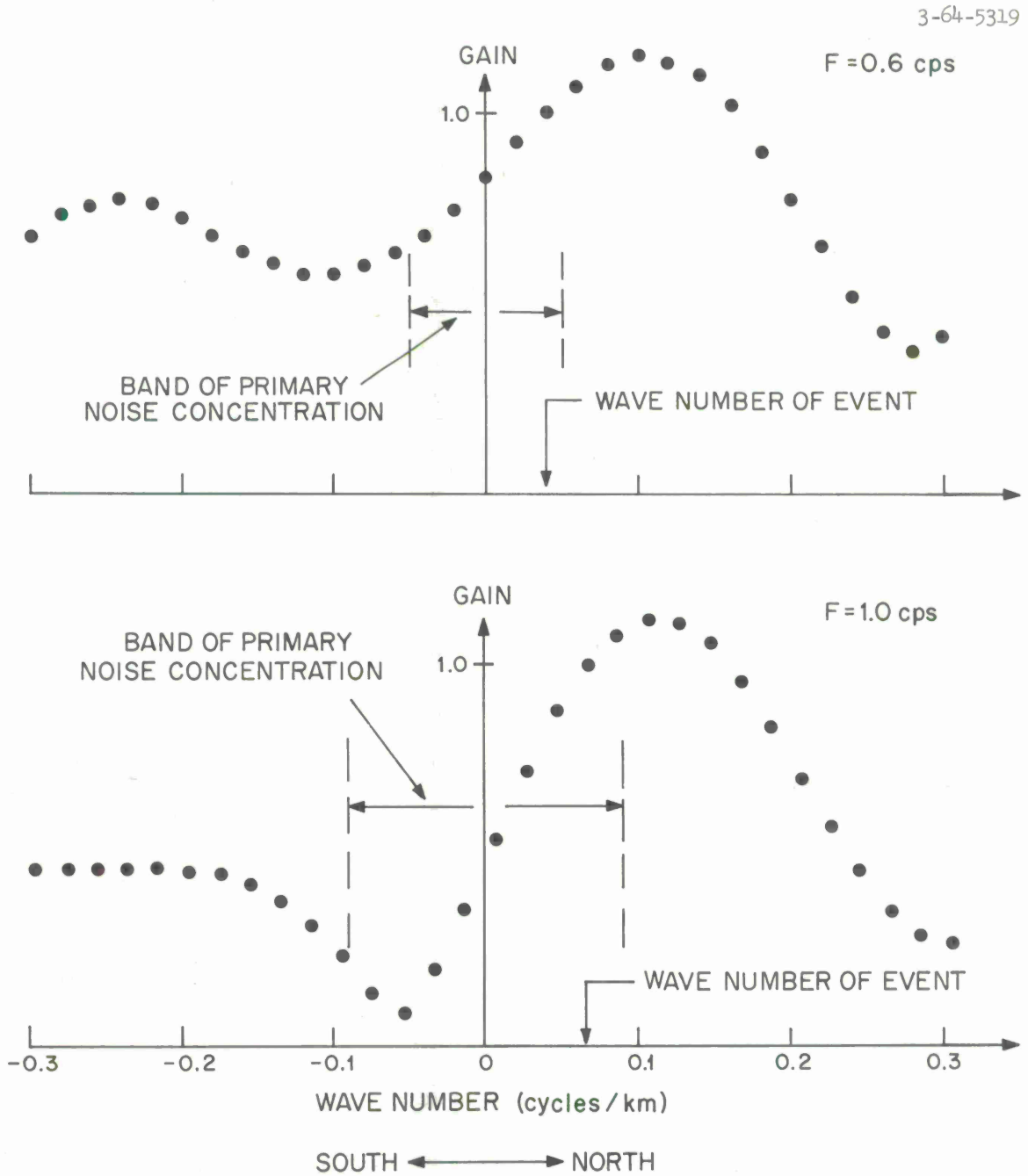

Figure 25. Frequency and Wave-Number Gains of Site B1, Input Traces Bandpass Filtered.

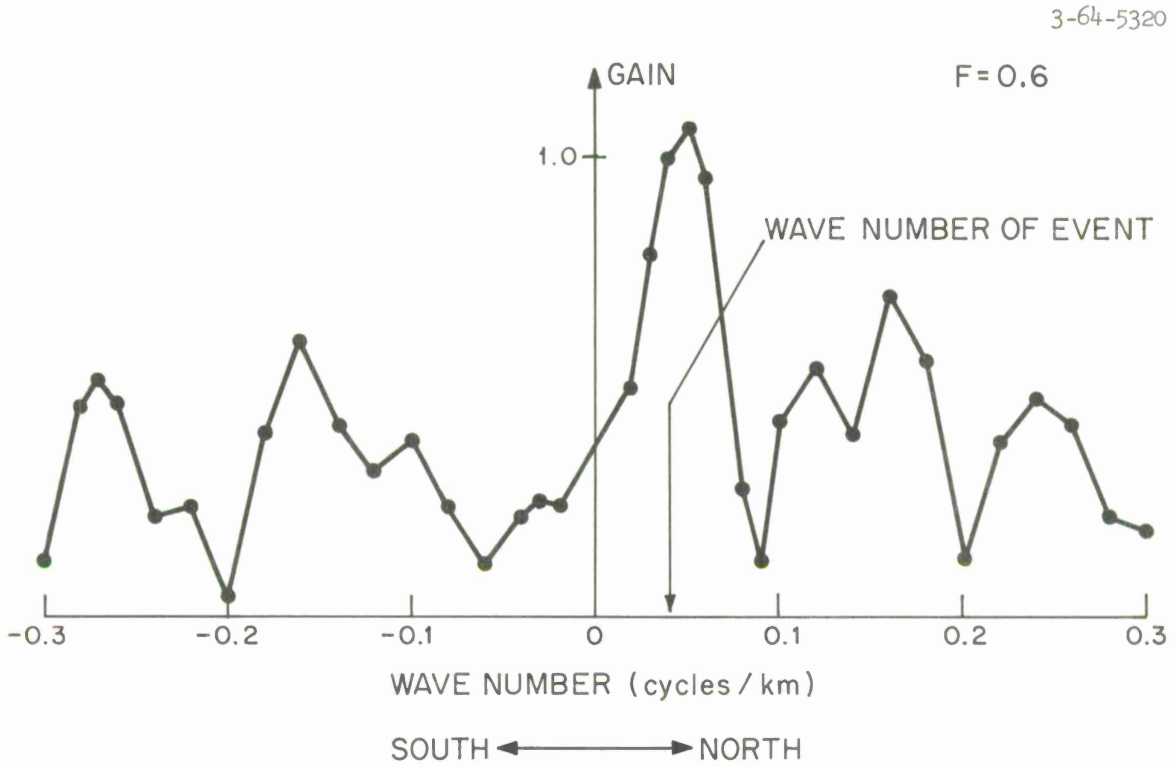

Figure 26. Frequency and Wave-Number Gains of 22 km Array, Input Traces Bandpass Filtered.

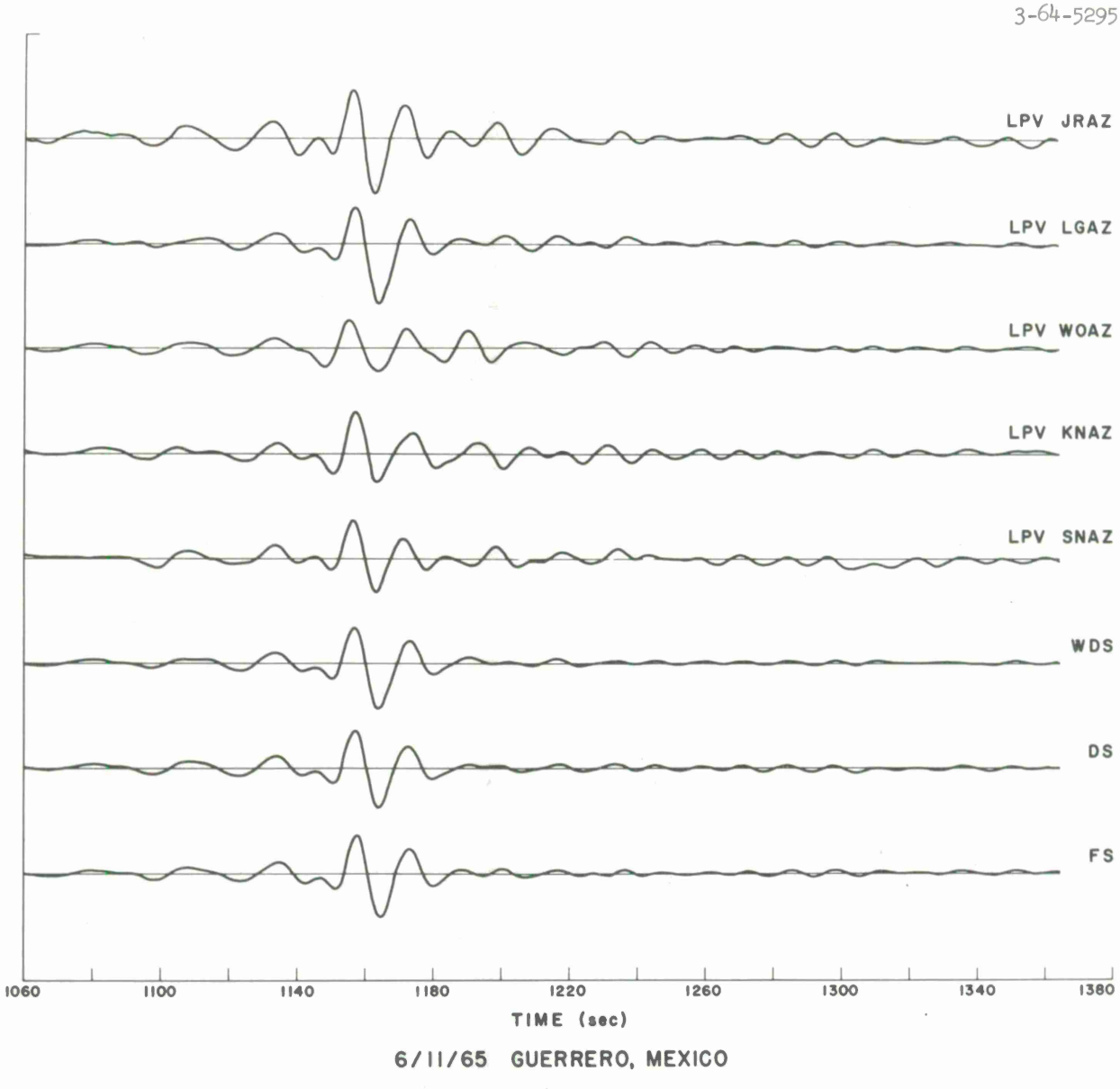

Figure 27. Processing Results for Long-Period Surface Waves.

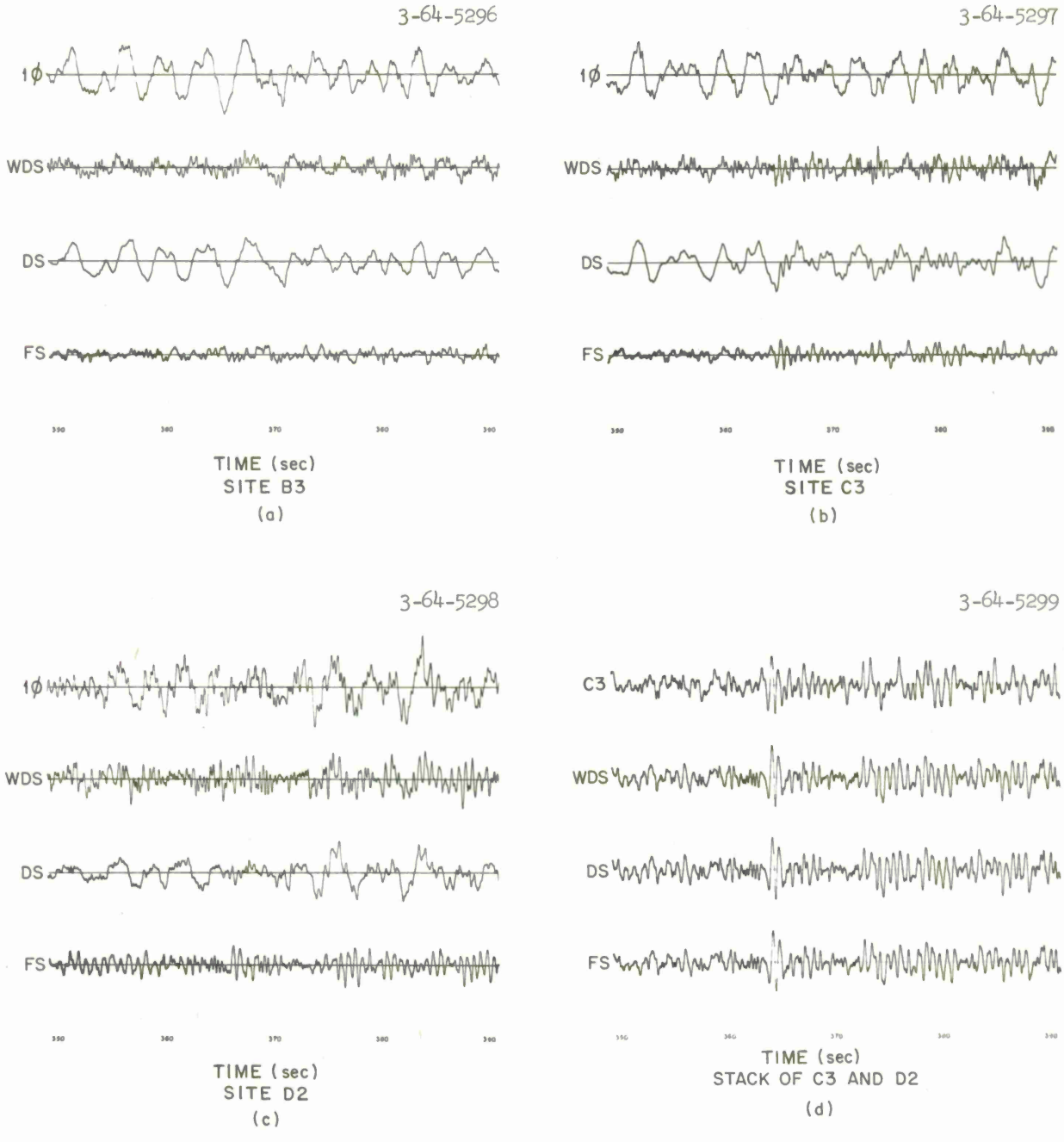

Figure 28. Weak Event Processing Results for the 12/11/65 Commander Islands Event, No Prefiltering.

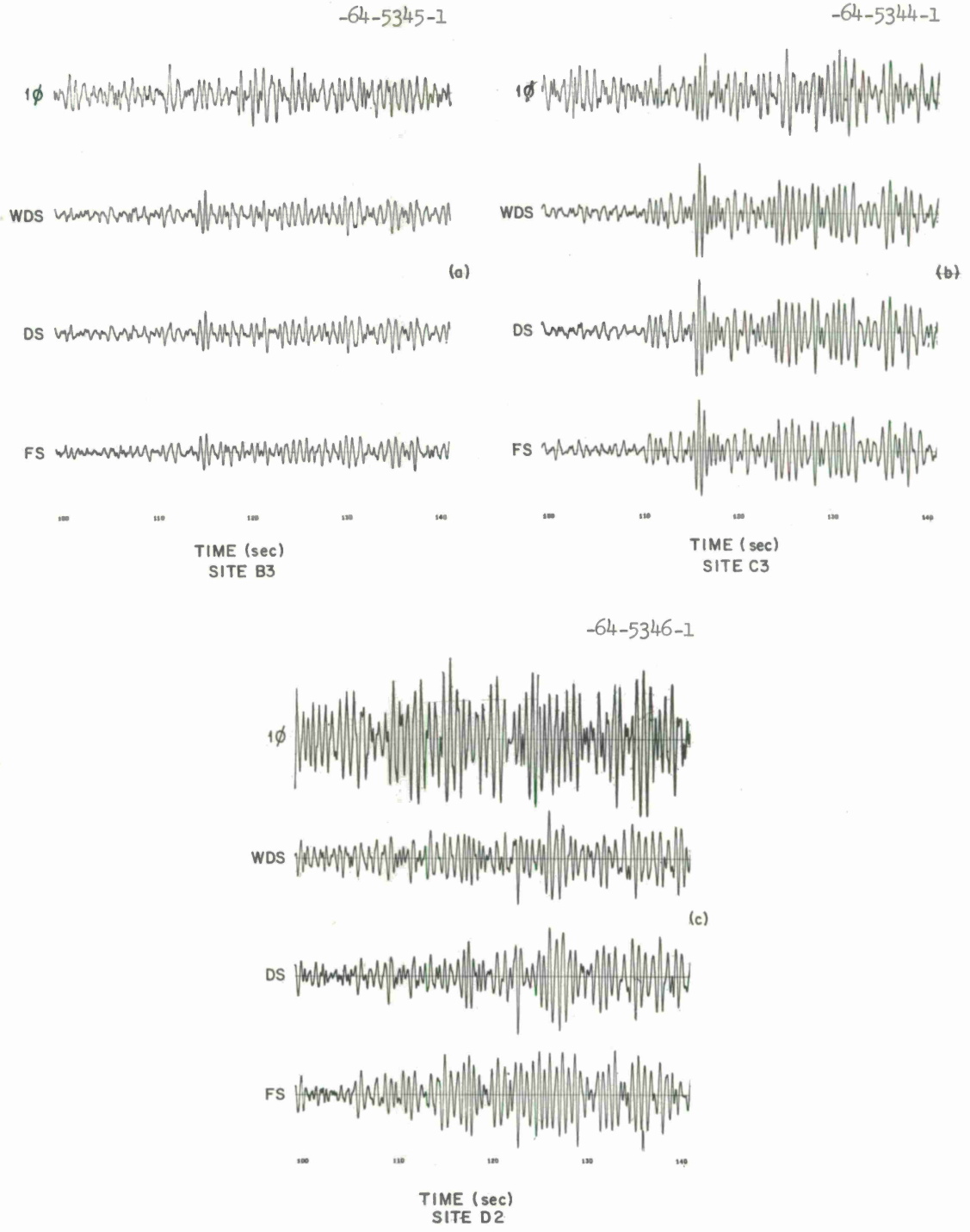

Figure 29. Weak Event Processing Results for the 12/11/65 Commander Islands Event, Input Traces Prefiltered, 1.15 to 3.5 cps.

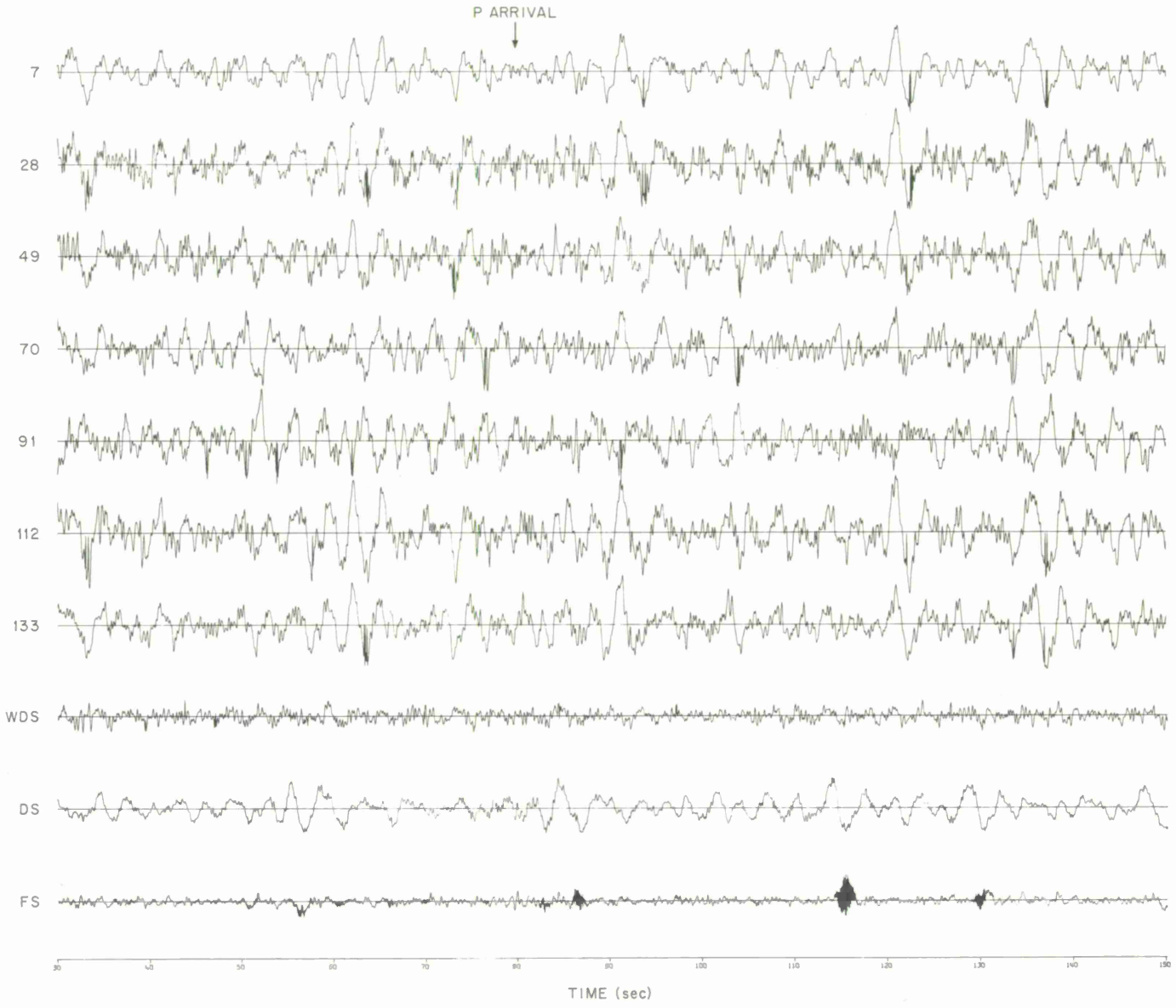

Figure 30. Weak Event Processing Results for the 10/1/65 Rat Island Event, Site B4.

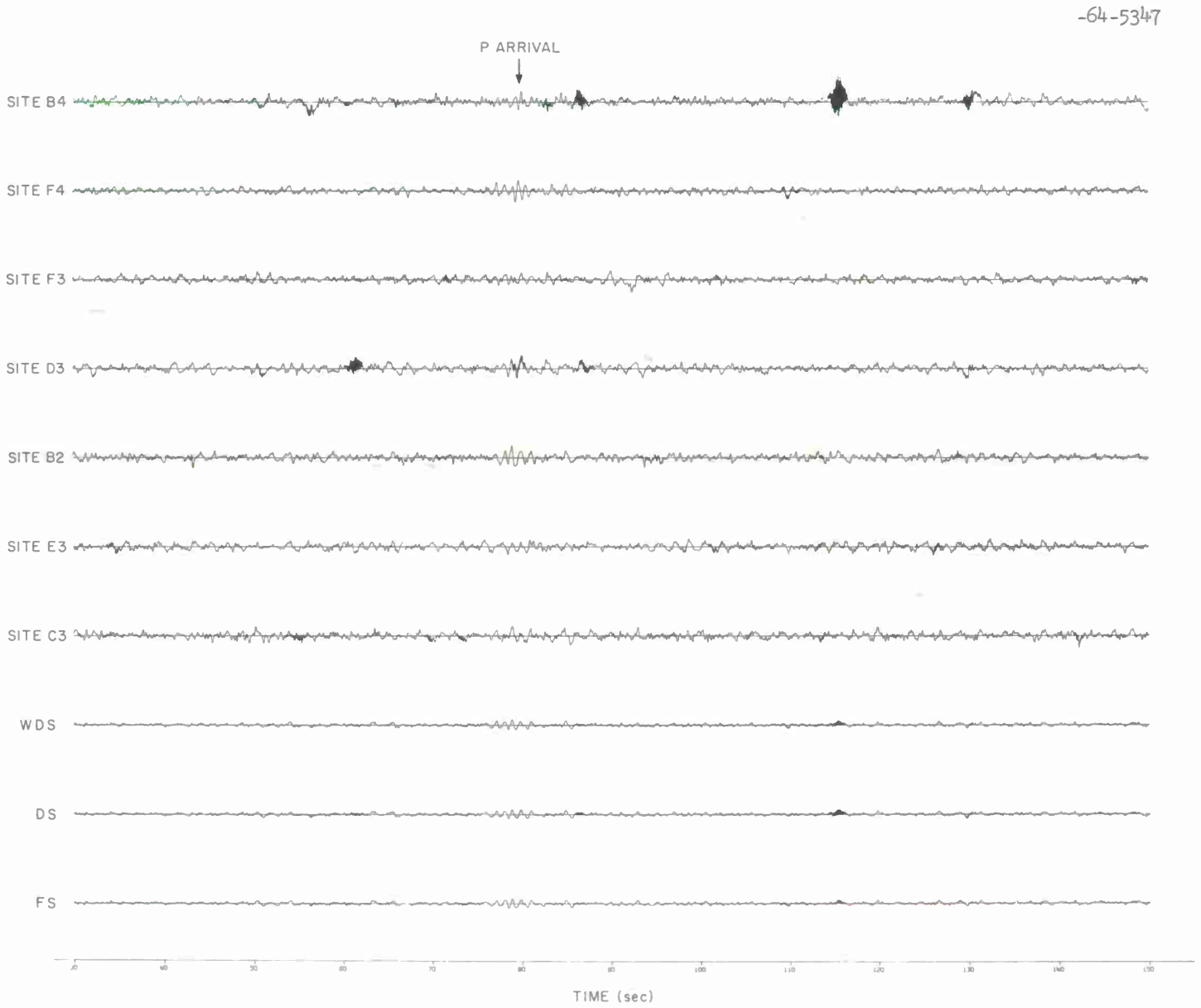

Figure 31. Stack of Seven FS Subarray Traces, 10/1/65 Rat Island Event.

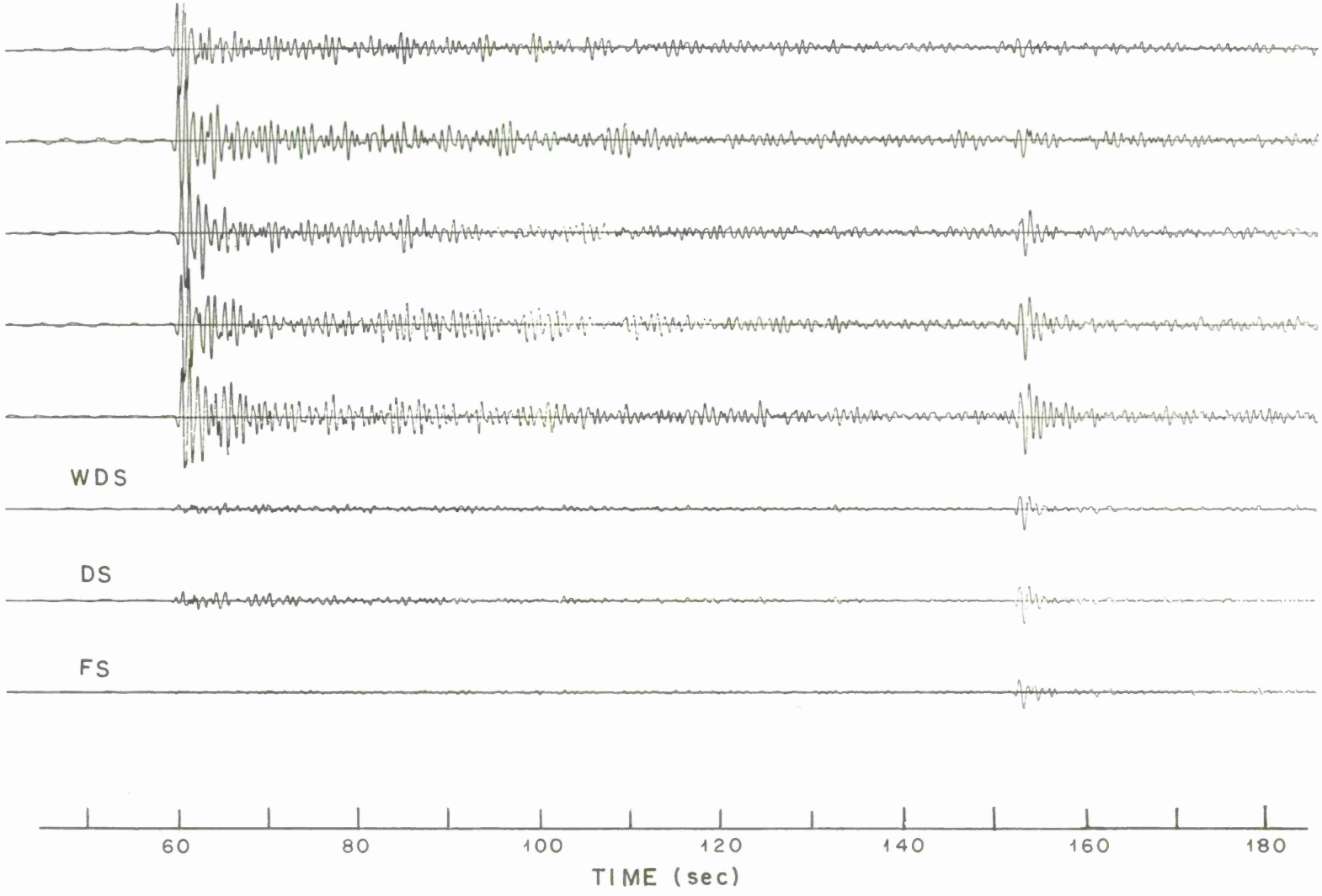

Figure 32. Suppression of P in favor of PcP.

DOCUMENT CONTROL DATA – R&D

(Security classification of title, body of abstract and indexing annotation must be entered when the overall report is classified)

1. ORIGINATING ACTIVITY *(Corporate author)*
Lincoln Laboratory, M.I.T.

2a. REPORT SECURITY CLASSIFICATION
Unclassified

2b. GROUP
None

3. REPORT TITLE
Off-Line Signal Processing Results for the Large Aperture Seismic Array

4. DESCRIPTIVE NOTES *(Type of report and inclusive dates)*
Technical Note

5. AUTHOR(S) *(Last name, first name, initial)*
Capon, Jack Greenfield, Roy J. Lacoss, Richard T.

6. REPORT DATE	7a. TOTAL NO. OF PAGES	7b. NO. OF REFS
11 July 1966	68	11

8a. CONTRACT OR GRANT NO.
AF 19(628)-5167
b. PROJECT NO.
ARPA Order 512
c.
d.

9a. ORIGINATOR'S REPORT NUMBER(S)
Technical Note 1966-37

9b. OTHER REPORT NO(S) *(Any other numbers that may be assigned this report)*
ESD-TR-66-249

10. AVAILABILITY/LIMITATION NOTICES
Distribution of this document is unlimited.

11. SUPPLEMENTARY NOTES
None

12. SPONSORING MILITARY ACTIVITY
Advanced Research Projects Agency, Department of Defense

13. ABSTRACT

The results of a series of off-line signal processing experiments are presented for the experimental Large Aperture Seismic Array (LASA) located in eastern Montana. In particular, the signal-to-noise ratio gains achievable by maximum-likelihood processing, as well as other simpler forms of processing, are given as a function of frequency, aperture, and number of sensors. A partial discussion of the physical characteristics of the noise field which led to these results is also presented.

The spurious precursor introduced by one form of signal processing, and shown to be caused primarily by the signal amplitude scatter within a subarray, can be effectively reduced by using amplitude equalization. The signal amplitude scatter within a subarray, and between subarrays, is thus found not to degrade seriously the performance of the signal processing. In fact, the scatter of amplitudes between subarrays, which is significantly larger than that within a subarray, is a definite asset.

It was found that the effectiveness of the processing depends not only on the array spatial filtering ability, but on differences in absolute level of the noises in the various sensors. Long-period array data from the extended TFO array were processed and showed roughly $\sqrt{N}$ improvement.

Our experience in processing a number of events is illustrated by a discussion of the results obtained on two particularly weak events with the maximum-likelihood filter. The average apparent magnitude of one event at LASA was 3.5, and that of the other was 4.0. It was found that the processing was capable of extracting both events from the background noise to the extent that they could be identified as earthquakes and not nuclear explosions. An experiment in suppressing large events that obscure simultaneous smaller events from other source regions is reported.

On the basis of these results, several recommendations concerning off-line and on-line processing methods and array geometry are given.

14. KEY WORDS

seismic array
signal-to-noise ratio
seismometer
Fourier transform
scattering
Vela-uniform
teleseism
sensors

Printed by
United States Air Force
L. G. Hanscom Field
Bedford, Massachusetts